Nina G. Jablonski
California Academy of Sciences, Golden Gate Park, San Francisco, California 94118-4599, U.S.A. E-mail: njablonski@calacademy.org

Meave G. Leakey and Christopher Kiarie
Department of Palaeontology, National Museums of Kenya, P.O. Box 40658, Nairobi, Kenya. E-mail: meaveleakey@swiftkenya.com; palaeontology@wananchi.com

Mauricio Antón
Departamento de Paleobiología, Museo Nacional de Ciencias Naturales, José Gutiérrez Abascal 2, 28006 Madrid, Spain. E-mail: MANTON@santandersupernet.com

Received 17 January 2002
Revision received 31 July 2002 and accepted 4 August 2002

Keywords: Cercopithecidae, Cercopithecinae, Papionini, Papionina, baboons, locomotion, opposability index, Pliocene.

A new skeleton of *Theropithecus brumpti* (Primates: Cercopithecidae) from Lomekwi, West Turkana, Kenya

A relatively complete skeleton of the fossil papionin, *Theropithecus brumpti*, from the site of Lomekwi, west of Lake Turkana, Kenya, is here described. The specimen, KNM-WT 39368, was recovered at the site of LO 5 (3°51′N and 35°45′E), from sediments dated to approximately 3·3 Ma. The skeleton is that of an old adult male and preserves a number of articulated elements, including most of the forelimbs and tail. The cranial morphology is that of a large, early *T. brumpti*, exhibiting a deep mandible with a deeply excavated mandibular corpus fossa, and mandibular alveoli and cheek teeth arrayed in a reversed Curve of Spee. The forelimb skeleton exhibits a unique mixture of characteristics generally associated with a terrestrial locomotor habitus, such as a narrow scapula and a highly stable elbow joint, combined with those more representative of habitual arborealists, such as muscle attachments reflecting a large rotator cuff musculature and a flexible shoulder joint. The forelimb of KNM-WT 39368 also presents several features, unique to *Theropithecus*, which represent adaptations for manual grasping and fine manipulation. These features include a large, retroflexed medial humeral epicondyle (to which large pronator, and carpal and digital flexor muscles attached) and proportions of the digital rays that denote capabilities for precise opposition between the thumb and index finger. Taken together, these features indicate that one of the earliest recognized representatives of *Theropithecus* exhibited the food harvesting and processing anatomy that distinguished the genus through time and that contributed to its success throughout the later Pliocene and Pleistocene. Based on the anatomy of KNM-WT 39368 and the known habitat preference of *T. brumpti*, the species is reconstructed as being a generally terrestrial but highly dexterous, very large-bodied, sexually dimorphic, and possibly folivorous papionin. *T. brumpti* was adapted for propulsive quadrupedal locomotion over generally even ground, and yet was highly adept at manual foraging. The estimate of 43·8 kg body mass for KNM-WT 39368 renders unlikely the possibility that the species, or at least adult males of the species, were highly arboreal. *T. brumpti*, as represented by KNM-WT 39368, is seen as a large, colorfully decorated, and basically terrestrial papionin that was restricted to riverine forest habitats in the Lake Turkana Basin from the middle to latest Pliocene.

Journal of Human Evolution (2002) **43,** 887–923
doi:10.1006/jhev.2002.0607
Available online at http://www.idealibrary.com on IDEAL®

Introduction

To a paleontologist, the value of an associated skeleton is inestimable. In primate paleontology alone, the study of specimens such as ''Lucy'' (AL-288-1, *Australopithecus afarensis*), the ''Turkana Boy'' (KNM-WT 15000, *Homo ergaster*), the 1958 skeleton of *Oreopithecus bambolii*, and the nearly complete skeleton of the giant East African

0047–2484/02/120887+37 $35.00/0

colobine monkey, *Paracolobus chemeroni* (KNM-BC 3), has demonstrated the superiority of complete over composite individuals in the elucidation of functional anatomical complexes, body size and proportions, and life history. Thus, even in the case of the present skeleton, in which the specimen does not represent a new taxon, we have a rare opportunity to investigate in detail the cranial and postcranial morphology of an undoubted individual extinct primate. This opportunity allows us to better illuminate the feeding and locomotor behaviors and ecological niche of one of the most distinctive fossil cercopithecids yet recognized.

The Old World monkey genus *Theropithecus* is one of the best known of fossil primate taxa, being recognized from thousands of specimens from sites in northern, eastern and southern Africa from the middle Pliocene through most of the Late Pleistocene. The most widespread and long-lived species of the genus, *T. oswaldi*, has also been identified from Pleistocene-aged sites outside of Africa, in India and Spain (Delson, 1993; Gibert *et al.*, 1995). *T. brumpti* was more localized in its spatial distribution, being recognized only from Pliocene-aged sites of the Lake Turkana Basin, namely, the Nachukui Formation of West Turkana and the Koobi Fora Formation of East Turkana in Kenya, and the Shungura Formation of the Omo in Ethiopia. At these sites, there is a temporal overlap between *T. brumpti* and *T. oswaldi* of about 1 Ma (Behrensmeyer *et al.*, 1997), but their relative frequencies during this interval are strikingly different. At the beginning of its tenure, in the middle Pliocene, *T. oswaldi* is barely discernible in the fossil record of the Turkana Basin, being greatly outnumbered by fossils of *T. brumpti*. Near the end of the Pliocene, about 1·9 Ma, however, the situation reversed, with *T. oswaldi* greatly outnumbering *T. brumpti* and the former on its way to being the common baboon from the later part of the Turkana Basin Pliocene and Pleistocene sequences. *T. brumpti* has been interpreted as occupying a riverine gallery forest habitat (Eck & Jablonski, 1987), whereas *T. oswaldi* is associated with more open habitats (Eck, 1987). The turnover from the dominance of one species to another appears to be a part of a more prevalent trend among the large mammals of the Turkana Basin that coincides with the transition from a river-dominated to a lake-dominated ecosystem (Feibel *et al.*, 1991). This transition involved a reduction in the number of species associated with forest-edge environments, and a corresponding increase in grazing herbivores to exploit the marshy grasslands of the delta and lake margins and the drier grasslands flanking them (Feibel *et al.*, 1991; Behrensmeyer *et al.*, 1997). The co-occurrence of fossils of *Theropithecus* with those of hominins at many African sites has provided a continuing stimulus for the study of the adaptations and evolutionary history of the genus, and the basis of models of hominin differentiation (Jolly, 1970; Foley, 1993).

Thanks to its generous fossil record and the molecular evidence of its phylogenetic relationships (see papers in Jablonski, 1993*b*; Disotell, 2000), the evolution of the genus is now fairly well understood. *Theropithecus* appears to be most closely related to baboons of the genus *Papio*, with the common ancestor of both having diverged from the common ancestor of *Mandrillus* and *Cercocebus*, probably in the early Pliocene (Disotell, 2000). These genera, commonly grouped together in the Subtribe Papionina, are believed to have originated in the early Pliocene from a species of *Parapapio* or other similarly generalized African cercopithecid. The fossil record has, unfortunately, shed little light on the mode or tempo of differentiation of the large papionins, or on their individual ancestries.

Theropithecus is represented in the fossil record by two distinct lineages, dominated respectively by the species *T. oswaldi* and *T. brumpti*. Delson (1993) has distinguished these taxonomically as the subgenera *T.* (*Theropithecus*) and *T.* (*Omopithecus*), respectively. The single extant species of the genus, *T. gelada*, has been accommodated in the former subgenus, but the nature of its phyletic relationship to other species in the genus remains unclear because of the absence of any relevant fossil evidence and its many distinctive autapomorphies. *T. gelada* lives on the high montane grasslands of central Ethiopia, and appears to represent a long-isolated sublineage within *Theropithecus*. The naming of species within the genus and the allocation of species to the genus have been controversial. Of relevance here is the debate that has surrounded the accommodation of species other than *T. brumpti* itself into the *T.* (*Omopithecus*) lineage. Eck & Jablonski (1984) argued for the inclusion of two Pliocene species, *Papio baringensis* and *P. quadratirostris*, into *Theropithecus* and specifically into the *T. brumpti* lineage. Delson and colleagues (Delson & Dean, 1993; Frost, personal communication) have argued that, while *P. baringensis* may be a theropith, *P. quadratirostris* is clearly not, and is better accommodated as a species of *Papio* (*Dinopithecus*). A detailed recitation of the arguments made by these authors is outside the scope of the present work, and readers are referred to the papers by Eck & Jablonski (1984) and Delson & Dean (1993) for this discussion.

The preservation of nearly complete forelimb skeletons for KNM-WT 39368 is fortuitous insofar as the forelimbs of cercopithecoids are widely recognized as being more informative of modes of locomotion and manipulation than the hindlimbs, which function mainly to provide propulsive thrust in locomotion. Thus, this account will focus primarily on a description and interpretation of the shoulder girdle and forelimb for *T. brumpti*.

Discovery and geological and paleoenvironmental contexts

One of the most productive regions for *Theropithecus* fossils representing both the *T. oswaldi* and *T. brumpti* lineages has been the Lake Turkana Basin. Located in the eastern Rift Valley of East Africa, the Lake Turkana Basin has provided a remarkable record of Miocene, Pliocene and Pleistocene fossils that has made a significant contribution to our current understanding of the tempo and mode of evolution of terrestrial African faunas (Coppens & Howell, 1985, 1987*a*,*b*; Feibel *et al.*, 1989; Harris 1981, 1983; Harris *et al.*, 1988*a*,*b*; Leakey *et al.*, 1996; Behrensmeyer *et al.*, 1997). Whereas much of this evidence has come from the Shungura and Koobi Fora Formations to the north and east of Lake Turkana respectively, the Nachukui Formation to the west, has made a significant contribution. The Nachukui Formation outcrops along a 10 km wide strip on the western shores of the lake between the settlements at Kalakol to the south and Lowarengak to the north. These deposits were initially investigated in the 1980s by the West Turkana Research Project as part of the National Museums of Kenya (NMK) field research program (Harris *et al.*, 1988*b*). Fieldwork over the subsequent decade led to the recovery of over 1000 specimens of 93 mammalian species. Geological studies revealed a sequence of tuffs interbedded in the 730 m of section, 23 of which had been previously recognized in the Koobi Fora and Shungura Formations. Recently field research in the Nachukui Formation was re-established by NMK teams led by Meave and Louise Leakey in collaboration with Frank Brown (University of Utah), who is studying detailed aspects of the geology.

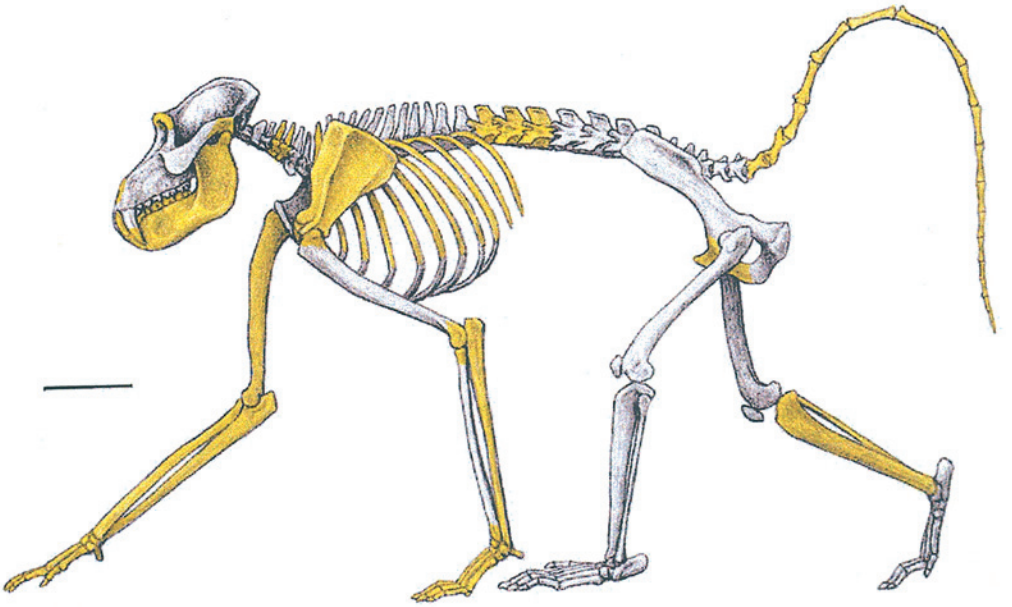

Figure 1. Reconstruction of the skeleton of KNM-WT 39368, with preserved elements indicated in yellow. Skull restoration based on male crania of *T. brumpti* from the Omo and West Turkana. Postcranial elements not preserved with the original specimen were reconstructed on the basis of other fossil *Theropithecus* and living papionins.

Within the Nachukui Formation (Harris *et al.*, 1988*a*,*b*), several sites documenting the earlier sediments in the Omo Group deposits are richly fossiliferous. One of these, LO 5, situated on the southern branch of the Laga Lomekwi, in the foothills of the Murua Rith range, was re-surveyed in 1998. Preliminary observations of the clasts in the fossiliferous conglomerates at LO 5 suggest that the site represents a paleostream channel that may have held drinking water; if this observation is borne out by further study, this may account for the concentration of bones at the site (Frank Brown, personal communication). Although many of the specimens found at LO 5 were fragmentary, at one locality, 3°51′N and 35°45′E, a fairly complete skeleton of *T. brumpti* was discovered by Wambua Mangoa. The specimen, which preserves a number of articulated elements (Figure 1), had begun to erode from the slope of a small hill, and was initially detected by a few fragments of the cranial and postcranial skeleton lying on the surface. Subsequent screening of the site revealed further skeletal elements *in situ* and an excavation followed which led to the recovery of an unusually complete monkey skeleton, catalogued as KNM-WT 39368. After retrieval of the surface fragments and commencement of the excavation, the disposition of the skeletal elements was revealed. The animal was discovered lying on its back, curled up with its head and hindlimbs nearer the surface, covering the more deeply buried forelimbs, thorax and tail. The absence of puncture or gnaw marks denotes that the animal was not the object of carnivore predation or scavenging. Death due to senescence or disease is far more likely, given the advanced state of wear of the dentition. The extraordinary completeness and articulation of the bones of KNM-WT 39368 raise questions over the deposition and fossilization of the specimen. Site LO 5 has not yielded other partial or

whole skeletons, and so one must invoke relatively uncommon taphonomic processes to account for the articulation of the forelimbs and preservation of fragile elements such as the ribs and scapula. The two most likely possibilities are that the carcass may have been partially mummified before deposition, or that the animal fell into the water and was rapidly covered with sediment thereafter.

The elements of the skeleton are mostly off-white, but are covered with a brown matrix veneer derived from the clayey sediments in which it was interred. The skeleton is not strongly mineralized, rendering the bones highly friable. Because of this, most of the skeletal elements suffered crushing during or after fossilization. The preparation of the skeleton, undertaken by one of us (CK), was extremely exacting and time-consuming, and required repeated sequences of gluing, re-positioning of elements, and stabilization.

The distribution of sedimentary facies within the Nachukui Formation suggests that, as today, the Labur and Murua Rith ranges formed the western margins of the basin and were drained by eastern-flowing rivers that fed into short-lived lakes, forerunners of the present lake, or into a major river system, the ancestral Omo River, flowing through the basin (Harris *et al.*, 1988; Leakey *et al.*, 2001). The site of LO 5 is situated close to the Marua Rith hills, and includes alluvial fan deposits brought in by rivers draining from the west and characterized by volcanic clasts derived from the Tertiary volcanics in the hills. These sediments include upward fining cycles of fine-grained clays, sandy silts and conglomerates which interfinger with sediments brought in by the ancestral Omo River drainage from the north. The section at LO 5 includes the Lomekwi and Kataboi Members which occur above and below the Tulu Bor tuff, respectively. The type section of the Lomekwi Member is 158·5 m thick. The upper boundary is defined as the Lokalalei Tuff (Tuff D) which has been dated at 2·52+0·05 Ma (Brown *et al.*, 1985). The *Theropithecus* skeleton was recovered from silty sands of the alluvial fan deposits 20–22 m above the Tulu Bor Tuff which has been correlated with the Sidi Hakoma Tuff of the Hadar Formation in Ethiopia (Brown, 1982) and is dated at 3·40+0·03 Ma (Walter & Aronson, 1993; Kimbel *et al.*, 1994). Assuming linear sedimentation rates between the two dated tuffs, the geologic age of the specimen can be estimated (by extrapolation based on the distance above the Tulu Bor Tuff), to be approximately 3·3 Ma.

The faunal assemblages from LO 5, as well as the geology, indicate a well-watered and well-vegetated paleoenvironment, consistent with other contexts in which *T. brumpti* has been found. A mosaic of habitats is indicated by the bovids, but with woodland- and forest-edge habitats dominating.

Description of KNM-WT 39368

KNM-WT 39368 represents the skeleton of an old adult male *T. brumpti*. The specimen comprises fragments of the cranium, a complete mandible, a partial sternum, fragmentary thoracic, lumbar and a complete sequence of caudal vertebrae, most ribs, the more or less complete forelimb skeletons from both left and right, including complete sets of carpals and digital rays preserved *in situ*, portions of the left os coxa, and bones of the right leg. No femora, tarsal bones or pedal digits were recovered. A complete list of the elements of the skeleton preserved in KNM-WT 39368 is provided in Table 1.

Cranium

Most of the cranium of KNM-WT 39368 appears to have disintegrated as a result of surface exposure and erosion. Fortunately, some fragments of diagnostic and functional

Table 1 The elements of the skeleton present in KNM-WT 39368

Element designation	Element identification
A	Rt digit II distal phalanx
B	Rt digit II middle phalanx
C	Rt digit II proximal phalanx
D	Rt digit III proximal phalanx
E	Rt digit III middle phalanx
F	Rt digit III distal phalanx
G	Rt digit IV proximal phalanx
H	Rt digit V metacarpal
I	Rt digit IV middle phalanx
J	Rt digit IV distal phalanx
K	Rt digit IV metacarpal
L	Rt digit III metacarpal
M	Rt digit II metacarpal
N	Rt digit I distal phalanx
P–Q	Rt sesamoids
R	Rt sesamoid with digit V metacarpal
S	Rt digit V proximal phalanx
T	Rt carpal
U	Rt lunate
V	Rt scaphoid
W	Rt ulna
X	Rt radius
Y	Lt digit III distal phalanx
Z	Lt digit II distal phalanx
AA	Lt digit II middle phalanx
AB	Lt sesamoid
AC	Lt digit III middle phalanx
AD	Lt digit III proximal phalanx
AE	Lt digit IV proximal phalanx
AF	Lt digit IV middle phalanx
AG	Lt digit IV distal phalanx
AH	Lt digit II proximal phalanx
AI	Lt digit IV metacarpal
AJ	Lt digit V metacarpal
AK	Lt digit V proximal phalanx
AL	Lt digit V middle phalanx
AM	Lt digit V distal phalanx
AN	Lt pisiform
AO	Lt triquetral
AP	Lt ulna
AQ	Lt hamate
AR	Lt sesamoid
AS	Rt rib fragment
AT	Lt tenth or eleventh rib fragment
AU	Lt eleventh or twelfth rib head
AV	Rt third or fourth fragment
AW	Rt rib head
AX	Lt lower rib fragment
AY	Lt eighth or ninth rib costal end
AZ	Rt seventh or eighth rib costal end
BA	Vertebra?
BB	Lt scapula
BC	Sternal body segment
BD	Rt second or third rib fragment
BE	Lt first or second rib

Table 1 *Continued*

Element designation	Element identification
BF	Lt eighth/ninth ribs (fused)
BG	Rt lower rib fragment
BH	Lt humerus
BI	Rt third or fourth rib
BJ	Rt rib fragment
BK	Rt eighth/ninth/tenth ribs (fused)
BL	Lt lower rib fragment
BM	Lt fourth or fifth rib fragment
BN	Rt first or second rib
BO	Bone fragment
BP	Lt capitate
BQ	Lt carpal
BR–BS	Rib heads
BT	Rt lower rib fragment
BU	Rib head
BV–BW	Caudal vertebrae
BX	First two caudal vertebra fused
BY–BZ	Sternal body segments
CA–CO	Caudal vertebrae
CP–CQ	Caudal vertebra fragments
CR	Sacrum dorsal fragment
CS	Rib fragments in bag
CT	Rt lower rib fragment
CU	Rt fourth or fifth rib fragment
CV	Lt second or third rib costal end
CW	Lt sixth or seventh rib
CX	Mandible
CY	Lt upper canine tip
CZ	Rt upper canine fragment
DA	Rt upper central incisor
DB	Rt upper lateral incisor
DC	Lt upper lateral incisor
DD	Upper premolar root?
DE	Upper molar crown and root broken
DF	Upper molar root in alveolus
DG	Upper molar root fragments
DH	Upper molar root fragments
DI	Upper molar root fragments
DJ	Upper molar root fragments
DK	Upper molar root fragments
DL	Lt glenoid fossa partial
DM	Lt supraorbital margin
DN	Occipital bone frag. near the inion
DO	Nasal bone fragment
DP	Lt premaxilla and maxilla fragment
DQ–DR	Muzzle fragments
DS–DT	Facial bone fragments
DU	Lt mastoid area fragment
DV–DW	Petrous temporal bone fragments
DX	Bag of cranial bone fragments
DY	Rt pubis and partial acetabulum
DZ	Iliac crest fragment
EA	Pelvic fragments in bag
EB	Axis odontoid process
EC	Third and fourth cervical vertebrae fused

Table 1 *Continued*

Element designation	Element identification
ED	Fifth and six cervical vertebrae lt zygapophyses fused
EE	First thoracic vertebra
EF	Thoracic vertebral body
EG–EI	Thoracic vertebra fragments?
EJ	Lumbar vertebrae, two fused
EK	Lumbar vertebra body
EL	Lower thoracic vertebral body
EM–EO	Lumbar vertebral body fragments
EP–ER	Lumbar neural spines
ES	Lumbar vertebrae fragments
ET–EU	Lower lumbar vertebrae transverse processes
EV	First caudal vertebra
EW–EX	Proximal caudal vertebrae
EY	Vertebrae fragments
EZ	Rt tibia
FA	Rt fibula
FB	Femoral head part?
FC	Rt clavicle
FD	Lt clavicle sternal head
FE	Lt humeral head crushed
FF	Lt humerus lateral epicondyle
FG	Lt radial head
FH	Humeral bone fragments
FI	Rt glenoid fossa of scapula
FJ	Rt acromion process
FK	Long bone fragments
FL	Bag of bone fragments
FM	Two rt sesamoid bones
FN	Three sesamoid bones
FO	Lt digit I proximal phalanx
FP	Lt lunate
FQ	Lt scaphoid
FR–FT	Lt carpals
FU	Rt digit I proximal phalanx
FV	Rt carpal
FW	Rt digit V middle phalanx
FX	Lt digit I distal phalanx

value were recovered as the result of careful surface collecting, sieving and identification. The most significant of these are listed below.

Maxillary dentition. The only piece of the maxillary dentition preserved is the tip of the left upper canine (KNM-WT 39368 CY). The anterior aspect of the tooth shows a strong developmental groove. The posterior (honing) aspect is very sharp. Although the base of the tooth was not preserved for measurement, the size of the canine tip, the great length of the lower P_3 honing facet, and the size of the lower canines (preserved in KNM-WT 39368 CX) suggest that the upper canine was very large.

Cranium. The only portions of the cranium preserved are a partial glenoid fossa of the left temporal bone (KNM-WT 39368 DL), the supraciliary margin and partial orbital roof of the left frontal bone (KNM-WT 39368 DM, Figure 2) and a fragment of the

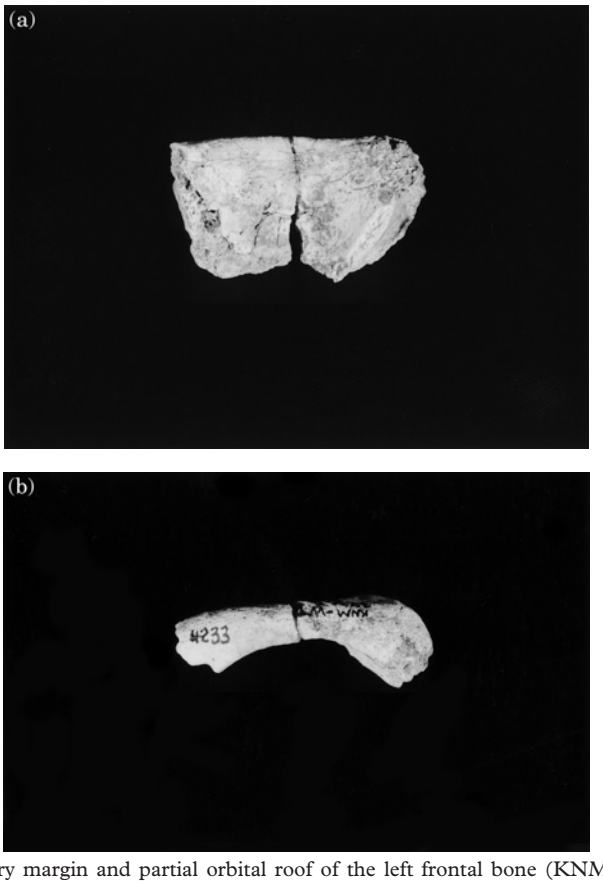

Figure 2. Supraciliary margin and partial orbital roof of the left frontal bone (KNM-WT 39368 DM); (a) superior view; (b) frontal view. Approximately life size.

Figure 3. Maxilla fragment (the left margin of the narial aperture) of KNM-WT 39368. Approximately life size.

muzzle preserving the left side of the narial aperture (KNM-WT 39368 DP, Figure 3). The partial glenoid fossa of the left temporal bone preserves the anterolateral surface only and adjacent surface of the temporal fossa. The orientation of the anterior margin of the

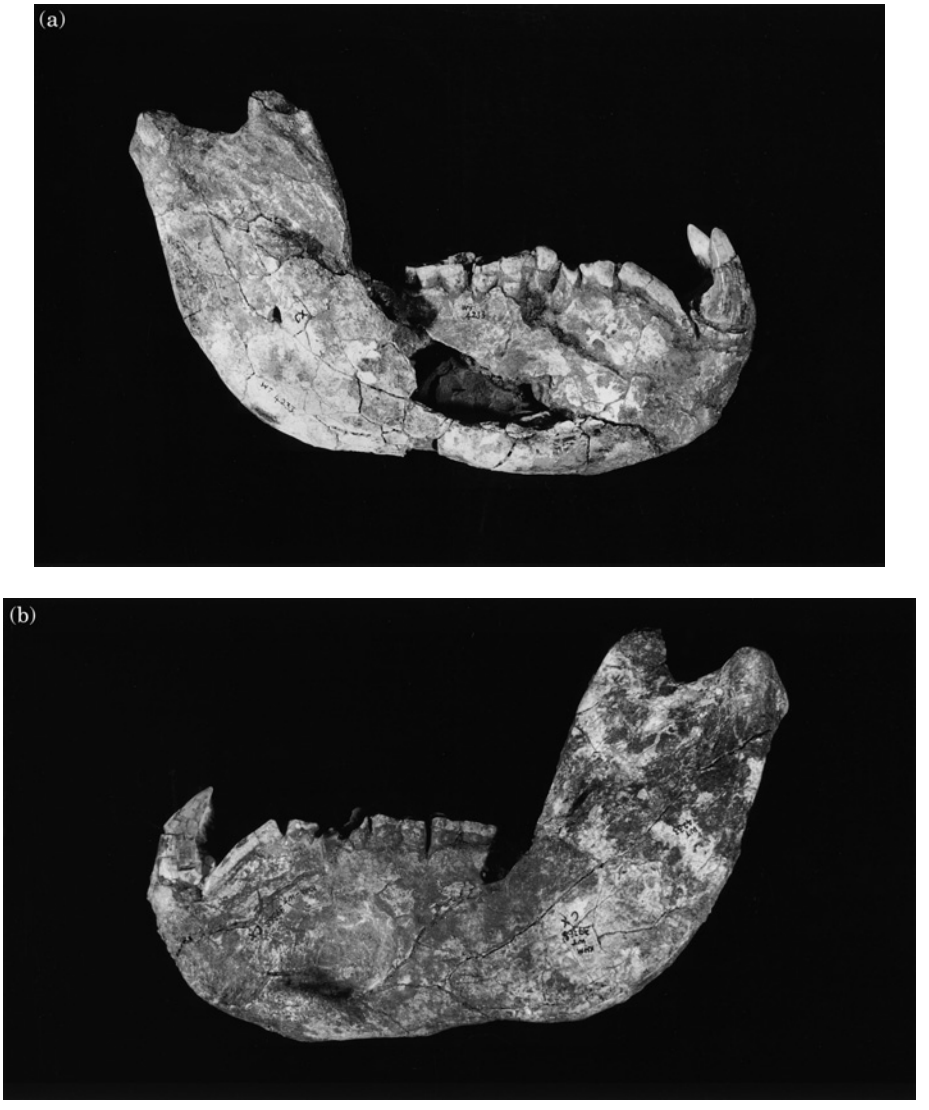

Figure 4. (a) and (b).

glenoid fossa is transverse. A lateral tubercle for attachment of the temporomandibular joint capsule is marked. The left frontal bone fragment was recognized by George Chaplin from a collection of sieving fragments. It represents a relatively thin orbital roof with a gracile supraciliary margin. A shallow supraciliary notch is preserved at the medial edge of the specimen. The superior surface of the bone is perforated by minute foramina, which transmitted blood vessels to and from hair follicles. The lateral aspect of the specimen preserves the anterior-most limb of the temporal line, indicating that the individual had an anteriorly thickened *M. temporalis* muscle. The muzzle fragment preserves a narrow strip of premaxilla medially and a larger area of maxilla laterally. The maxilla bears numerous small foramina and striae and appears to have been highly

Figure 4. (c)

Figure 4. Mandible (KNM-WT 39368 CX). (a) right lateral view; (b) left lateral view; (c) occlusal view. Approximately one-half life size.

vascularized. The small size of the fragment precludes reconstruction of the narial aperture or the contour of the muzzle. Another probable muzzle fragment, KNM-WT 39368 DS, shows extensive evidence of surface vascularization, but, unfortunately, cannot be placed in its correct anatomical position and is not illustrated here.

Mandible and mandibular dentition

The mandible (KNM-WT 39368 CX, Figure 4) contains a complete lower dentition except for the right lower lateral incisor that apparently was lost *ante mortem*. The diagnosis of sex and age for KNM-WT 39368 was based on the mandibular dentition, which is clearly that of an old adult male. The mandibular corpora have been compressed together during fossilization, bringing the tooth rows in close proximity and giving the bone an unnaturally narrow appearance. Matrix has not been removed from between the mandibular corpora, precluding measurement of the thickness of the mandibular symphysis. All the teeth are heavily worn, especially those on the left side. The dimensions of all the measurable teeth are given in Table 2. The canines are heavily worn, but were long and slender during life. The protolophid of the right M_1 is worn below the cervix and the hypolophid only slightly less so. The left M_1 appears to have worn through at the waist and broken into mesial and distal halves, resulting in the exposure of the pulp chamber of the hypolophid. Because of the advanced state of dental wear, very little of the cusp morphology of the molars can be described, except for the M_3s. On these teeth, the main cusps are large, broad-based, relatively steep-sided and the hypoconulids are large. The mandibular corpora themselves are deep and display deep, anteriorly situated fossae of the mandibular corpora. The fossae are ovate and are deepest at the level of the P_4 and M_1. On the right, the fossa of the mandibular corpus has been crushed and is absent posteriorly to the level of the retromolar fossa. The inferior borders of the mandibular corpora are thickened into

Table 2 **Dimensions of the mandible and mandibular teeth of KNM-WT 39368 CX**

Measurement	mm
Lower first incisor buccolingual width	6·3
Lower second incisor mesiodistal length	3·5
Lower second incisor buccolingual width	6·1
Lower canine mesiodistal length	16·1
Lower canine buccolingual width	15·8
Lower third premolar mesiodistal length	25·7
Lower third premolar buccolingual width	7·6
Lower fourth premolar mesiodistal length	8·9
Lower fourth premolar buccolingual width	7·1
Lower first molar mesiodistal length	12·7*
Lower first molar buccolingual width (mesial lophid)	8·8*
Lower first molar buccolingual width (distal lophid)	9·7*
Lower first molar buccolingual width (waist)	8·4*
Lower second molar mesiodistal length	14·7
Lower second molar buccolingual width (mesial lophid)	12·6
Lower second molar buccolingual width (distal lophid)	13·5
Lower second molar buccolingual width (waist)	10·9
Lower third molar mesiodistal length	18·6
Lower third molar buccolingual width (mesial lophid)	13·1
Lower third molar buccolingual width (distal lophid)	11·8
Lower third molar buccolingual width (waist)	10·8
Lower canine to lower third molar length	89·4
Lower third premolar to lower third molar length	76·8
Lower fourth premolar to lower third molar length	55·5
Lower first molar to lower third molar length	46·3
Lower tooth row length (to alveolare)	93·6
Lower tooth row length (to bite point)	92·3
Lower bicanine breadth	29·5*
Lower incisive alveoli width	16·6*
Mandibular condyle length (anteroposterior dimension)	14·6
Mandibular condyle width (mediolateral dimension)	24·9
Mandibular condyle to the mesial edge of lower first molar	119·4
Mandibular condyle to the distal edge of lower third molar	77·3
Moment arm of the masseter	93·9
Moment arm of the temporalis	29·4
Mandibular length (to alveolare)	169·8
Mandibular length (to bite point)	166·4
Mandibular corpus height (between lower first and second molars)	49·1
Mandibular symphysis length	64·3

*Indicates an estimated value.

All dental measurements represent maximum dimensions; definitions of mandibular measurements follow Jablonski (1993*a*).

anterior ridges that are particularly prominent at the level of the P_4. These substantial ridges contribute to the depth of the mandibular corpus fossae. Single, large, elliptical mental foramina perforate the anterior surface of the ridges under the lower P_3–P_4 junction. Proceeding rostrally, the ridges of the inferior corpus thin under the lower P_3 and develop a rugose inferior surface that leads to the rugosities of the mental eminence. The mental symphysis is very long, with its inferior shelf extending posteriorly to the level of the lower P_4. The rugosities that cover its rostral surface form a narrow inverted "V" shape as one views the symphysis from the front. The alveoli of

mandibular teeth, as well as the remnants of the teeth themselves, describe the reversed Curve of Spee that is seen in most specimens of *Theropithecus* throughout time (Eck & Jablonski, 1987; Jablonski, 1993*a*). The mandibular ramus is inclined at an angle of approximately 120° relative to the base of the mandibular corpus. The mandibular condyle is robust and deep in an anteroposterior direction. The articular surface extends from its superior aspect along the posterior surface of the condyle for approximately 14 mm, describing an articular contour that is common in cercopithecoids that demonstrate open-mouthed gape displays (Jablonski, 1993*a*). The coronoid process is raised only slightly above the level of the mandibular condyle.

Axial skeleton

A large number of ribs are preserved, although the poor condition of most of them precludes their identification by number. Three sternal body segments, KNM-WT 39368 BC, BY and BZ, are also preserved. The skeleton also comprises several vertebrae, but the identification of some elements has been hampered by poor preservation. Two complete cervical vertebrae are preserved together in a block of matrix (KNM-WT 39368 EC). One complete superior thoracic vertebra, T1 or T2, is also preserved (KNM-WT 39368 EE). The lumbar vertebrae are in poor condition and cannot be clearly identified. Most remarkable is the preservation of a complete series of 19 tail vertebrae, from the most proximal (KNM-WT 39368 BX) to the most distal (KNM-WT 39368 CO). The tail vertebrae are characteristic of those of modern long-tailed cercopithecids and show no evidence of extreme muscularity. The lengths of the caudal vertebrae are given in Table 3. The thoracic vertebra and ribs of KNM-WT 39368 are shown in Figure 5.

Table 3 Lengths of the caudal vertebrae of KNM-WT 39368

Specimen number (suffix to KNM-WT 39368)	Caudal vertebra number	Lengths (mm)
BX	1 and 2 (fused)	76·0 (combined length)
CA	3	51·0
CB	4	55·0
BW	5	53·0
BV	6	51·0
CC	7	47·5
CD	8	45·5
CE	9	41·5
CF	10	37·5
CG	11	32·5
CH	12	28·5
CI	13	25·0
CJ	14	21·5
CK	15	16·2
CL	16	13·8
CM	17	10·9
CN	18	8·9
CO	19	7·0

The vertebrae are listed in sequence from most proximal (KNM-WT 39368 BX) to most distal (KNM-WT 39368 CO).

Forelimb skeleton

Clavicle. The left clavicle is preserved (KNM-WT 39368 FC). Its natural curvature has been exaggerated greatly during fossilization, precluding determination of the element's length or natural degrees of torsion or curvature. The sternal end of the clavicle is large and has a quadrangular outline. The medial portion of the shaft is oval in cross-section. The shaft thins and broadens laterally into a craniocaudally flattened acromial end.

Scapula. A complete left scapula is preserved (KNM-WT 39368 BB, Figure 6), as well as the glenoid fossa (KNM-WT 39368 FE, Figure 6) and acromion (KNM-WT 39368 FT) from the right. The scapula is subisoceles in shape (*sensu* Roberts, 1974). The vertebral (medial) border is thin, relatively long and slightly convex, supporting a large

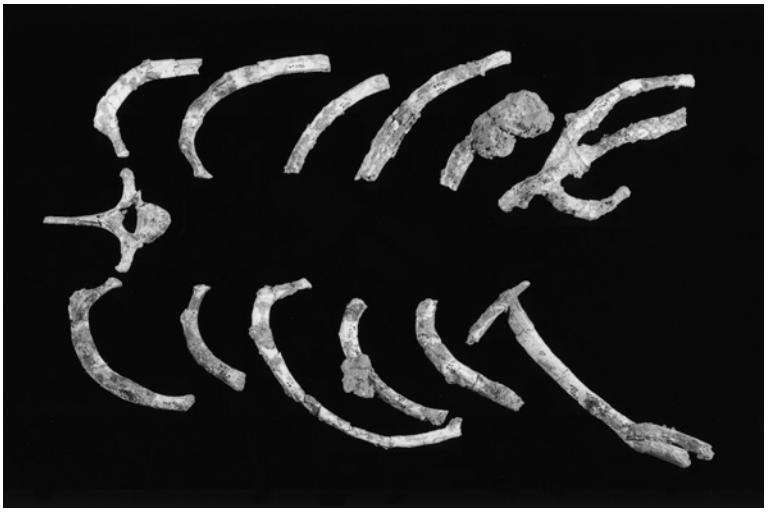

Figure 5. The thoracic vertebra (T1 or T2) and ribs of KNM-WT 39368. Clots of matrix can be seen adhering to the surfaces of several of the bones. Approximately one-fourth life size.

area for the attachment of *M. serratus anterior*. The lateral (inferior or axillary) border is a complex region rather than a simple edge. The medial aspect of the lateral border and the inferomedial angle of the scapula's dorsal surface is occupied by the moderately sized attachment area of *M. teres major*. The central and lateral portions of the lateral border are dominated by a sharp crest that extends medially from the infraglenoid tubercle and extends roughly two-thirds along the length of the lateral border. This crest contributes to the formation of a broad axillary sulcus whose ventral margin consists of a thickened keel or scapular pillar (Olivier & Depreux, 1954) that separates the lateral border from the costal surface. The surface of this sulcus is interpreted as providing attachment for an accessory slip of the *M. subscapularis* (Olivier & Depreux, 1954; Birchette, 1982). The superior border of the scapula is evenly thin and rises from the base of the coracoid to its most superior point, at about the midpoint of the margin. From this point medialward the superior margin runs transversely to intersect the vertebral border. The costal aspect of the scapula describes an undulating, concave surface that accommodated the attachment of a large *M. subscapularis*. The supraspinous fossa is shaped roughly like a long rectangle that has had its superior and lateral corner obliquely trimmed. The floor of the supraspinous fossa is on the same plane as that of the infraspinous fossa. The infraspinous fossa is roughly triangular in outline and constitutes more than two-thirds of the bone's dorsal surface area. The scapular spine is very deep for most of its length of the element, and has a smooth, narrow edge. Its base is oriented almost perpendicular to the blade. Unfortunately, the spine was crushed superiorly during or after fossilization, rendering difficult an accurate appreciation of its depth and contour. The acromion is short, stout and roughly quadrangular, being slightly flattened craniocaudally. Laterally, the lateral border recurves sharply toward the superior margin of the glenoid fossa. The coracoid process rises from a wide base, which is the continuation of the scapula's superior border. The process itself is oblong and lies at an angle of about 70° to its base, with its major axis directed ventrolaterally. The glenoid fossa (cavity) is symmetrically piriform, with a

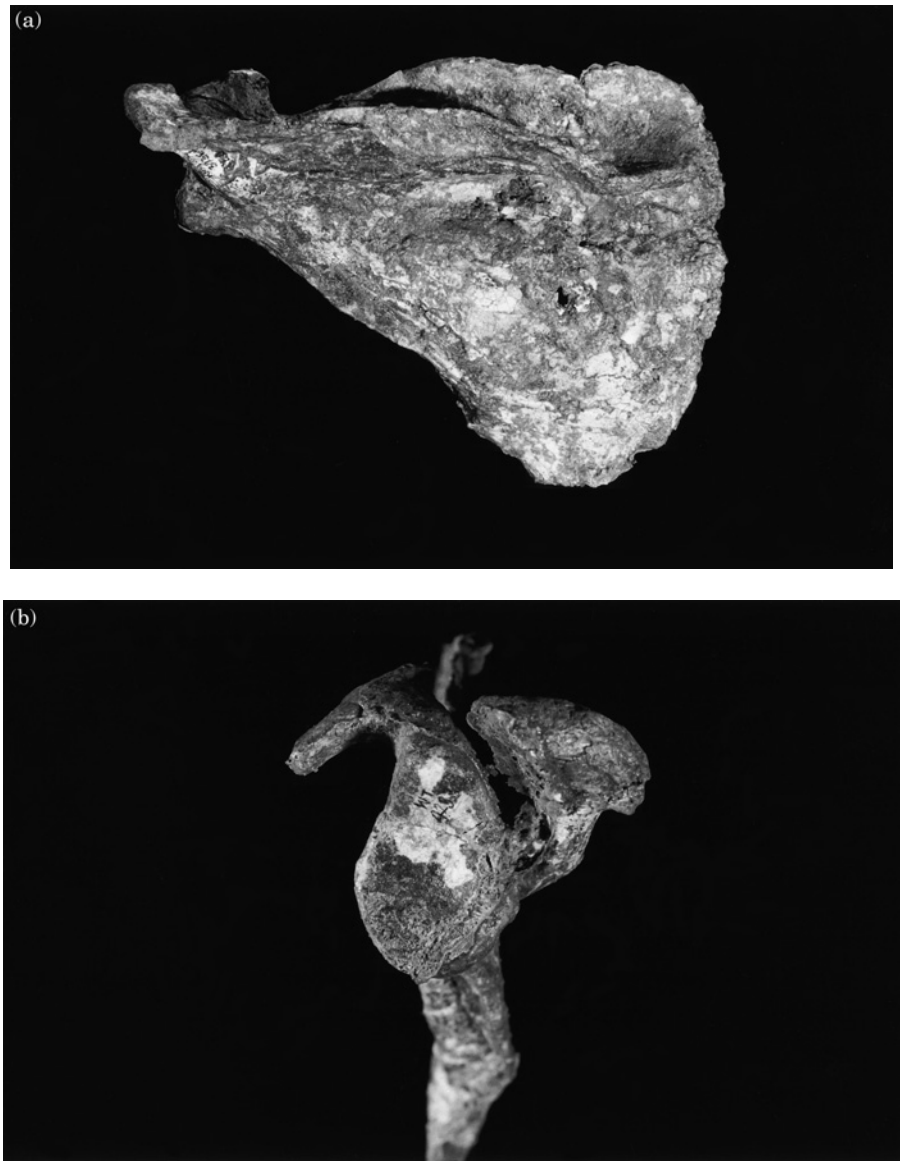

Figure 6. The left scapula, KNM-WT 39368 BB; (a) dorsal view. Approximately one-half life size; (b) view of the glenoid fossa of the right scapula, KNM-WT 39368 FE, approximately life size.

well-delimited periphery. The superior margin of the fossa protrudes slightly past the deepest point of the fossa's concavity, creating a slight cranial lip. The orientation of the fossa is lateral when the vertebral border is oriented along the craniocaudal axis. The greatest functional thickening of the scapula is along its inferior border, especially in the area interpreted as being the attachment area for the accessory slip of *M. subscapularis*. The dimensions of the scapula, as well as those of most of the other preserved fore- and hindlimb elements of KNM-WT 39368, are given in Table 4.

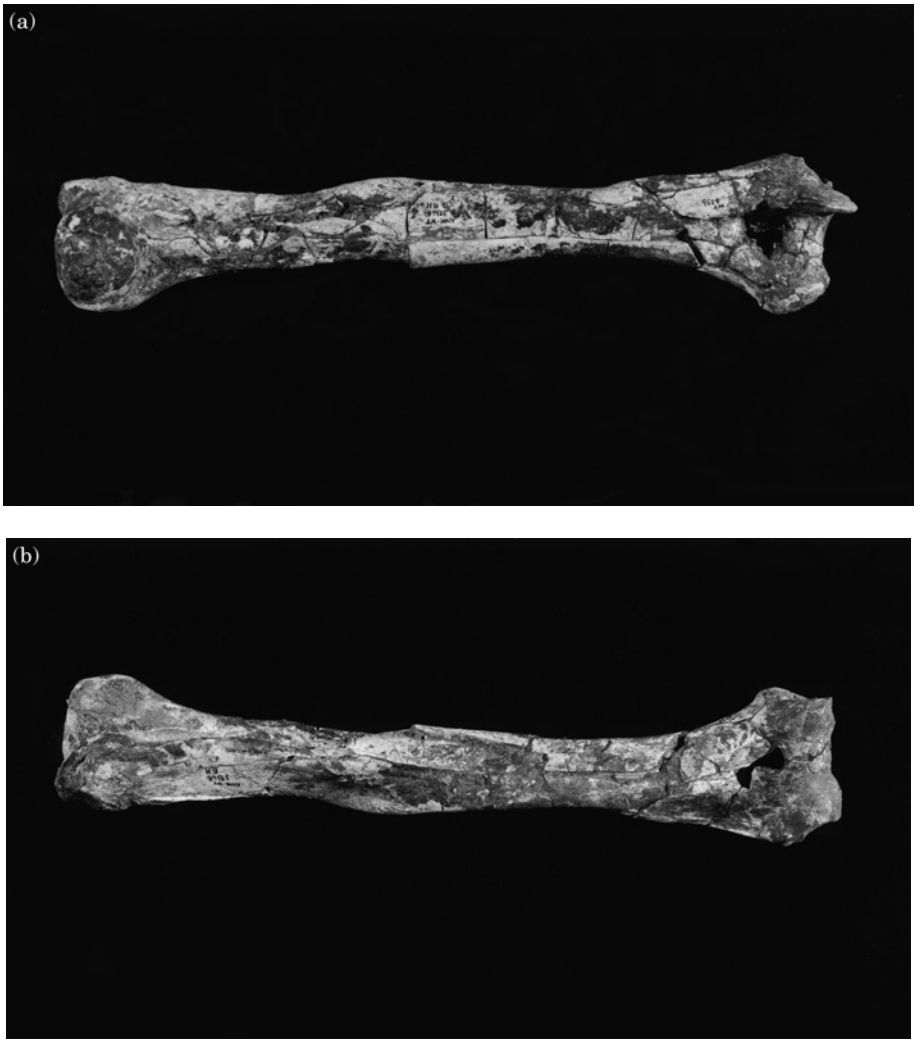

Figure 7. The right humerus, KNM-WT 39368 BH; (a) posterior view; (b) anterior view. Note the pathological enlargement of the lateral lip of the trochlea. Slightly less than one-half life size.

Humerus. A complete right humerus (KNM-WT 39368 BH, Figure 7), a left humeral head (KNM-WT 39368, FE) and left lateral epicondyle (KNM-WT 39368 FF) are preserved. The right humerus was crushed extensively, especially in midshaft, but has been reconstructed to restore the bone's natural contours. The nearly hemispherical head of the humerus is directed dorsally and slightly craniad. It is slightly wider in its mediolateral dimension than it is long. The greater tuberosity is broad, but does not extend superiorly past the level of the humeral head. A large, pitted facet for the insertion of *M. infraspinatus* is well demarcated on the lateral surface of the tuberosity, but a well-defined facet for the insertion of *M. supraspinatus* on its superior aspect is lacking. Ventrally, this tuberosity has a sharp, elevated edge that forms the proximal end of the lateral lip of the intertubercular groove. The lesser tuberosity lies

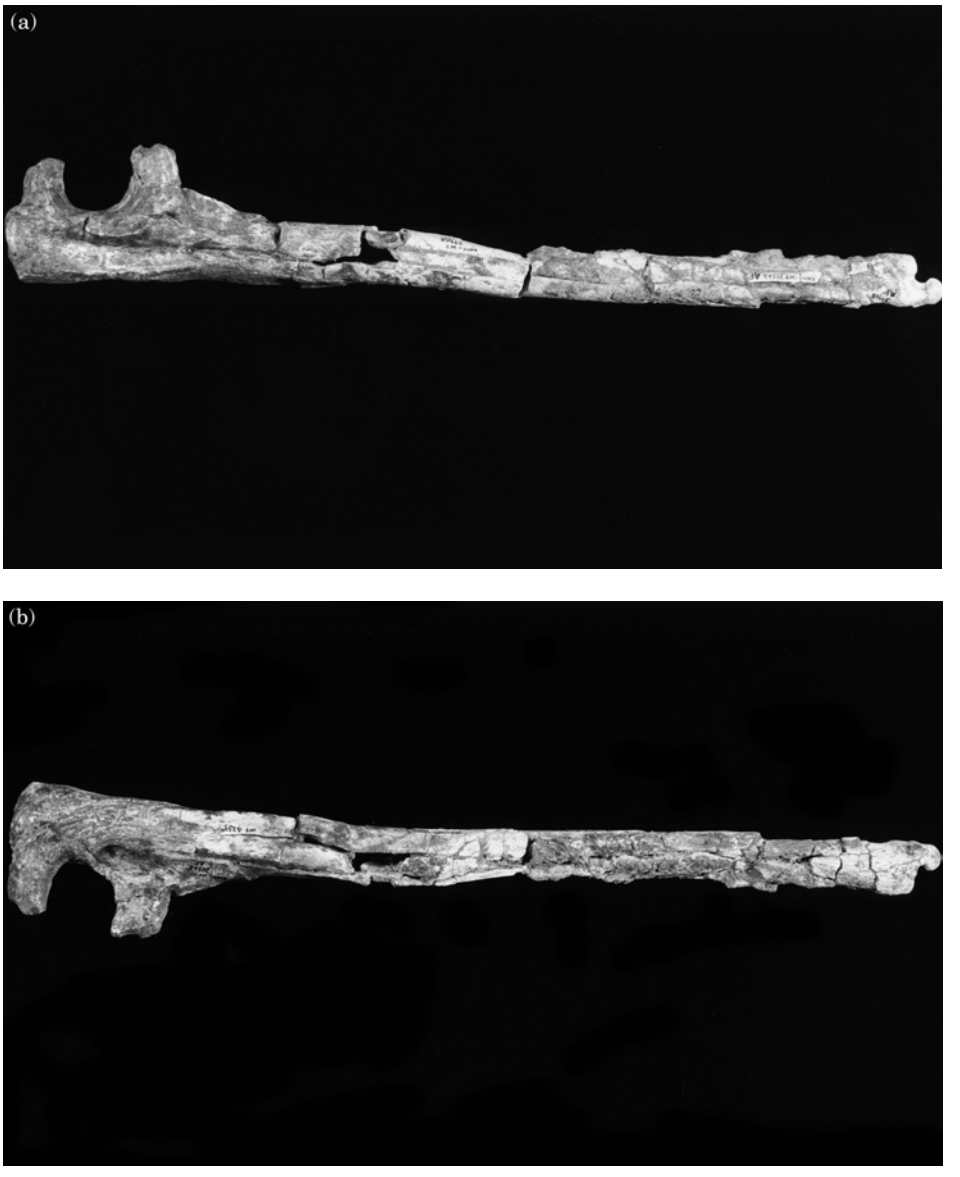

Figure 8. The left ulna, KNM-WT 39368 AP; (a) medial view; (b) lateral view. Note the pathological exaggeration of the margins of the sigmoid notch, probably due to osteoarthritis. Slightly less than one-half life size.

below the level of the humeral head. A curved, smooth area on its medial surface marks the attachment area of *M. subscapularis*. The ventral surface of the tuberosity forms a rounded edge to the proximal end of the medial lip of the intertubercular groove. The groove itself is deep and narrow, and remains well defined below the surgical neck. The deltoid crest, which is a continuation of the lateral lip of the intertubercular groove, is very strongly developed, and extends to midshaft. A large delto–triceps–brachialis crest runs distally on the ventral surface from the level of the surgical

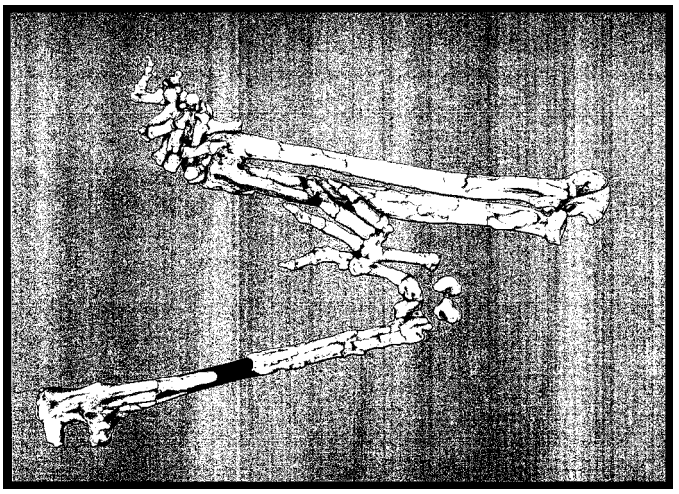

Figure 9. Drawing of the articulated forelimb skeletons of KNM-WT 39368 as they were found *in situ* at Lomekwi site LO 5. Drawing by Peter Gaede. Approximately one-fourth life size.

neck and then winds around the lateral aspect of the shaft until it intersects first the intradeltoid crest and then the deltoid crest at midshaft. The insertion for *M. deltoideus* on the humeral shaft is large and rugose at its margins. The shaft of the humerus is very straight; unfortunately, damage to the bone at midshaft precludes assessment of the shape of the midshaft cross-section. The lateral supracondylar ridge (supinator crest) is raised and develops into slight flange that curves posteriorly from the lateral epicondyle to the lateral aspect of the distal shaft. The medial epicondyle is large and strongly dorsiflexed, exhibiting almost no true medial projection. An elliptical facet on its distomedial surface accommodated the attachments of strong tendons of the wrist and digital flexors. The lateral epicondyle presents a large muscular attachment area and a prominent tubercle for the attachments of *Mm. extensor carpi radialis brevis* and *extensor digitorum communis*. The capitulum exhibits a characteristically semi-ovoid articular surface that extends considerably ventrally of the concave surface of the trochlea. The details of the true trochlea are difficult to discern because of damage, but on the ventral surface of the distal humerus it is narrower than the capitulum. Viewed posteriorly, the trochlea is a deep and relatively narrow gutter, the medial margin of which develops a large trochlear flange. The distal extremity of this feature has, unfortunately, been damaged and its full extent cannot be assessed. Despite this damage, the trochlear flange still extends distally beyond the lowest point on the capitulum and appears to have undergone pathological enlargement during life, possibly as the result of osteoarthritis. The olecranon fossa is damaged, but appears to have been deep and relatively narrow.

Ulna. Both ulnae are preserved, but suffered from crushing. Fortunately, neither bone was badly deformed and both have been nearly completely reconstructed. On the right (KNM-WT 39368 W, Figure 8), the proximal ulna is a separate element while the distal ulna has been preserved in its *in situ* position along with the right distal radius and right carpus (Figure 9). The left ulna (KNM-WT 39368 AP) is preserved as a separate element. The proximal end of the ulna is distinguished by a retroflexed

Table 4 Dimensions of the preserved elements of the appendicular skeleton of the KNM-WT 39368

Measurement	Value (mm)
Scapular length (transverse dimension)	135·1
Scapular width (vertebral border length)	106·6
Glenoid fossa length	31·0
Glenoid fossa width	21·9
Angle of the scapular spine to the glenoid fossa	88°
Angle of the lateral (inferior) border to the glenoid fossa	127°
Angle of the lateral (inferior) border to the scapular spine	37°
Humeral head diameter (superior-inferior dimension)	27·3
Humeral head diameter (medial-lateral dimension)	31·7
Humeral length (including trochlear flange)	230·9
Humeral length (to trochlea)	223·8
Distance from the superior margin of the humeral head to the distal-most extent of the deltoid tuberosity	112·3
Biepicondylar breadth	47·5
Distal humeral articular surface width	36·3
Medial epicondylar width (measured on the ventral surface)	5·8
Medial epicondylar width (measured on the dorsal surface)	15·4
Trochlear breadth (ventral)	14·5*
Trochlear breadth (dorsal)	15·3*
Capitulum breadth	22·8
Lateral epicondylar breadth (dorsal)	12·8
Capitulum anteroposterior diameter	12·1
Humeral midshaft diameter (dorsoventral)	17·8*
Humeral midshaft diameter (mediolateral)	24·2
Ulnar length (including styloid process)	260*
Olecranon length	20·4
Sigmoid (trochlear) notch length	18·1
Sigmoid (trochlear) notch breadth (at its midpoint)	21·8
Coronoid process protrusion from the base of the sigmoid notch	18·4
Proximal ulnar breadth at the radial notch	28·1
Ulnar midshaft diameter (dorsoventral)	13·9
Ulnar midshaft diameter (mediolateral)	11*
Angle of inclination of the sigmoid notch relative to the long axis of the ulna	17°
Angle of inclination of the olecranon relative to the long axis of the ulna	48°
Radial length	233*
Radial midshaft diameter (dorsoventral)	11·1*
Radial midshaft diameter (mediolateral)	17·5
Radial neck length (to the inferior margin of the bicipital tuberosity)	46·9
Radial neck diameter (dorsoventral)	15·6
Radial head diameter (mediolateral)	19·5
Radial head diameter (mediolateral)	22·3
Tibial length	219·4
Tibial midshaft diameter (dorsoventral)	26·5*
Tibial midshaft diameter (mediolateral)	13·6
Fibular length	203

*Indicates an estimated value.
Measurements of the proximal ulna follow Conroy (1974) and Jolly (1972).

olecranon of moderate length that develops a rounded, superomedially directed flange. This flange develops into a rounded crest that extends distally down the posterior aspect of the shaft for over one-third of its length. The proximal end of the olecranon, including its extensive flange and crest, are rugose and clearly accommodated the insertion of a large *M. triceps brachii* tendon. The medial aspect of the olecranon

overshadowed by the flange is a deep fossa that accommodated the origins of *Mm. flexor carpi ulnaris* and *flexor digitorum profundus*, responsible for radial deviation of the wrist and flexion of the fingers, respectively. The anconeal and coronoid processes are robust and project strongly ventrally, contributing to the creation of a constricted sigmoid (trochlear) notch. In ventral view, the sigmoid notch is narrow and resembles a twisted parallelogram, with the sides and the articular surfaces of the anconeal and coronoid processes directed craniolaterally. The ventral surface of the sigmoid notch folds around the medial and lateral surfaces of the anconeal process and the medial surface of the coronoid process. The enlargement of the coronoid process and the extensive folding over of the articular surface of the sigmoid notch onto the medial surface of the process is asymmetrically developed, being considerably larger on the left side than on the right. This is interpreted here as being another indication of bony pathology due to osteoarthritis. The radial notch is shallow, slightly concave centrally, and projects slightly laterally. The surface area of the notch cannot be assessed on the right due to damage and has been expanded by the pathological enlargement of the coronoid process on the left . The shaft of the ulna is relatively straight, showing only a slight medialward bowing at midshaft. The interosseous crest is visible as a blunt ridge beginning immediately distal to the radial notch. Its distal extent cannot be assessed because of extensive damage to the bone at midshaft. The supinator fossa, which is interposed between the interosseous crest and the anterior border of the ulna, is shallow. On the lateral surface of the ulna between the interosseous crest and the posterior border is a broad fossa that accommodated the attachments of the long pollical flexor and extensor and that of *M. extensor digiti secundi et tertii proprius*. The styloid process is stout, rounded and only slightly projecting. (Measurements of the angular inclination of the olecranon process inclination and sigmoid notch are included in Table 4.)

Radius. The complete right radius (KNM-WT 39368 X) is preserved, but its distal end remains in an *in situ* block with the right distal ulna and right carpus (Figure 9). On the left, only the radial head (KNM-WT 39368 FG) and distal epiphysis (KNM-WT 39368 AP) are preserved. As with the other forelimb long bones, the radius has been crushed, but well reconstructed. The shaft appears to have been straight. The head is nearly circular in outline, showing only a slightly greater mediolateral than dorsoventral dimension. The shallow, centrally located depression on its superior surface accommodated the humeral capitulum. The medial edge of the head is slightly higher than is the lateral, resulting in a slight mediolateral obliquity to its orientation. The neck of the radius, although somewhat damaged, is robust, and appears exceptionally thick at the proximal end of the bicipital (radial) tuberosity. The bicipital (radial) tuberosity is large in area, but the details of its surface cannot be discerned because of damage. The size of the tuberosity suggests a large insertion for *M. biceps brachii*. The interosseous crest is prominent and is aligned approximately with the medial border of the radial tuberosity. The anteromedial surface of the radius is bounded by the anterior border and the interosseous crest. In ventral view, the concavity of this surface has been exaggerated by post mortem crushing. The radial styloid process is sharply pointed, but is not strongly distally projecting.

Carpus. The identification of all the individual carpal bones from the left side has proved highly problematic, except for the large scaphoid (KNM-WT 39368 FQ) and lunate (KNM-WT 39368 FP). These bones

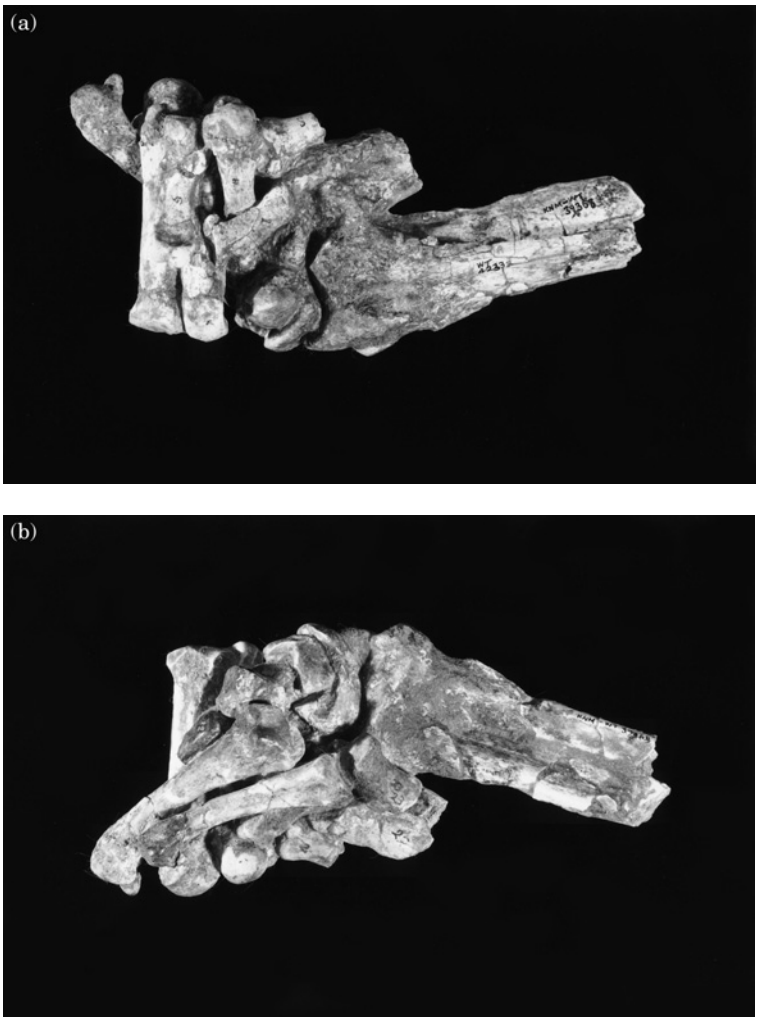

Figure 10. Posterior (a) and anterior (b) views of the right wrist area. Aproximately one-half life size.

can also be seen interposed between the distal radius and the metacarpals in the block of articulated elements from the right side (see Figure 10).

Metacarpals. The metacarpals and phalanges of both hands are complete and well preserved (Figure 11). Having been found articulated *in situ* (and mostly preserved in that condition on the right side), there has been no question as to the proper identification of digital number. The specimen numbers and dimensions of these elements are given in Table 5. The description here is based on the anatomy of the elements of the left hand, which were carefully disarticulated and labeled during preparation. In their morphology and proportions, the metacarpals and phalanges of KNM-WT 39368 closely resemble those of *T. gelada*. Metacarpal I is a long, slender bone. Its expanded proximal articular surface is ovate, concave and slightly expanded ventrally to fit the articular process of the trapezoid.

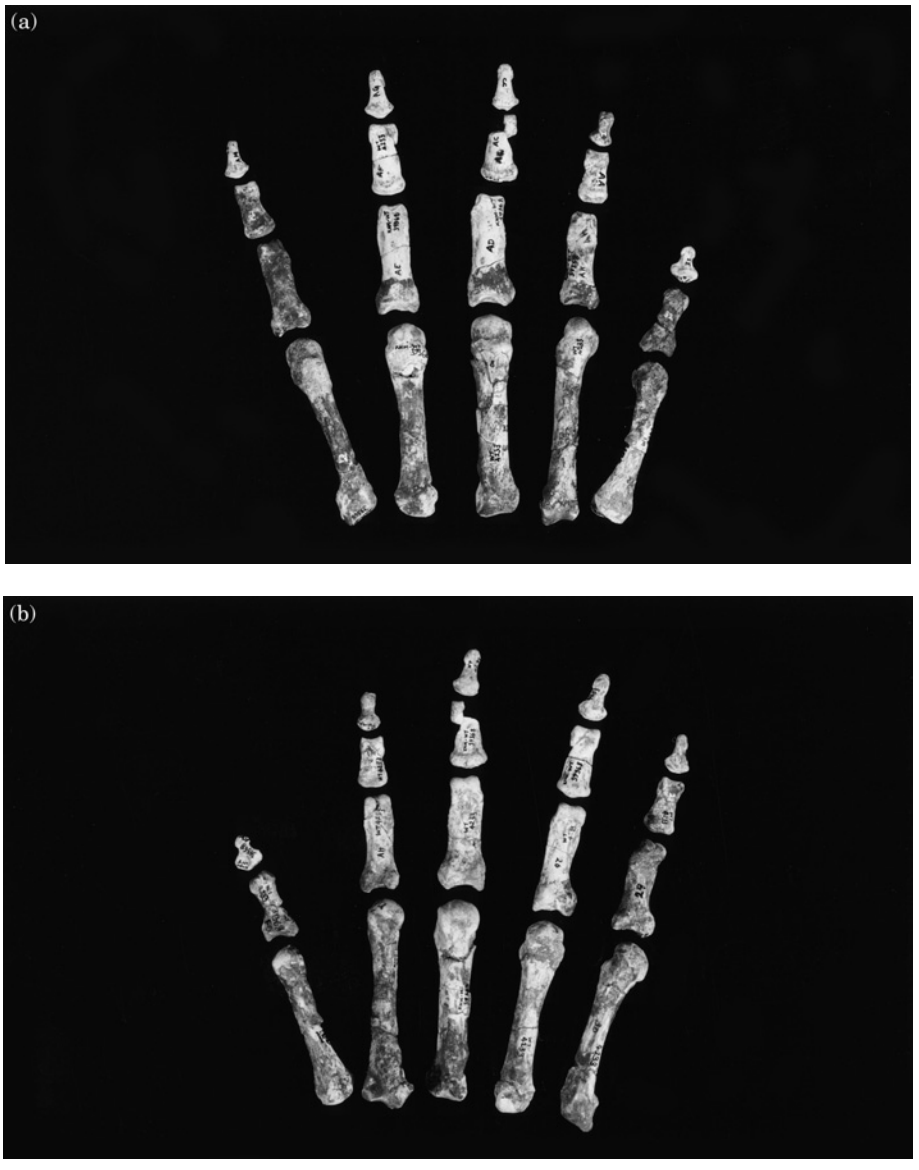

Figure 11. Posterior (a) and anterior (b) views of the left manus of KNM-WT 39368. Bony elements shown approximately one-half life size, with spaces between the bones exaggerated in order to clearly display the anatomy.

The head of the first metacarpal is small, rounded and slightly mediolaterally compressed. Metacarpal II is a robust bone with a stout base, which is dominated by the articular facet for the trapezium. Like metacarpal I, its head is small, rounded and mediolaterally compressed. Metacarpal III is virtually identical in length to metacarpal II, but exhibits a significantly more robust shaft. Its base bears a broad, flat facet for articulation with the capitate, and its head is broad and rounded. Metacarpal IV, only

Table 5 Lengths of the metacarpals and phalanges of the left manus of KNM-WT 39368

Specimen number (suffix to KNM-WT 39368)	Element	Measurement (mm)
BS	Ray I metacarpal	40·1
FO	Ray I proximal phalanx	17·7
FX	Ray I distal phalanx	9·0
BU	Ray II metacarpal	50·5
AH	Ray II proximal phalanx	23·7
AA	Ray II middle phalanx	13·0
Z	Ray II distal phalanx	9·4
BJ	Ray III metacarpal	48·9
AD	Ray III proximal phalanx	27·8
AC	Ray III middle phalanx	16·5*
Y	Ray III distal phalanx	11·3
AI	Ray IV metacarpal	47·1
AE	Ray IV proximal phalanx	27·2
AF	Ray IV middle phalanx	17·8
AG	Ray IV distal phalanx	11·7
AJ	Ray V metacarpal	47·1
AK	Ray V proximal phalanx	23·5
AL	Ray V middle phalanx	14·1
AM	Ray V distal phalanx	9·4

*Estimated due to damage.

slightly shorter than metacarpal III, also exhibits a robust shaft. Its base is narrow and dominated by the dorsoventrally oriented facet for articulation with the hamate. Its head is somewhat narrower than that of metacarpal III. Metacarpal V, only slightly shorter than IV, is, again, a robust bone. The mediolaterally beveled base bears a poorly defined facet for articulation with the pisiform. The head is as described for metacarpal IV. The shafts of all of the metacarpals are round in cross-section and are straight.

Phalanges. The proximal phalanx of digit I has been slightly crushed, but the details of its anatomy have not been obscured. It bears a broad base and a slender shaft that is elliptical in cross-section. Viewed from the side, a slight dorsoventral curve of the shaft can be discerned. The proximal phalanges of digits II–V exhibit broad bases and flattened, slightly dorsoventrally curved shafts. Of the middle and distal phalanges, only the distal phalanx of digit I warrants comment. This small bone has a broad, flattened base that tapers distally to a dorsoventrally compressed and mediolaterally rounded terminus; in appearance the bone closely resembles that of *T. gelada*.

Hindlimb skeleton

Os coxa. The largest piece of the pelvis preserved is from the left side and which comprises most of the left pubis (KNM-WT 39368 DY). The specimen has been badly crushed and distorted. The obturator foramen is preserved, but its natural outline cannot be accurately reconstructed. Only a small portion of the anterior aspect of the acetabulum is preserved and the diameter of the fossa cannot be estimated. A large collection of pelvic fragments were recovered at LO 5, but could not be accurately re-assembled.

Tibia. Only the right tibia (KNM-WT 39368 EZ, Figure 12) is preserved. The shaft of the bone has been crushed and reconstructed. The general anatomy of the tibia is conservative among cercopithecids, and the present specimen conforms to this pattern. The superior articular surface of the tibia is oriented nearly perpendicular to the long axis of the shaft. The lateral aspect of the lateral tibial condyle has been partially eroded and displaced slightly superiorly during or after fossilization. Despite this, it is still clear that the lateral aspect of the tibial plateau was smaller in area and oriented on a more superior plane than the medial. The tubercle for attachment of the cruciate ligaments is strongly raised. A posterior enlargement of the lateral condyle may be due to the fusion of the sesamoid bone of the lateral head of *M. gastrocnemius* to that process. The tibial shaft is robust dorso

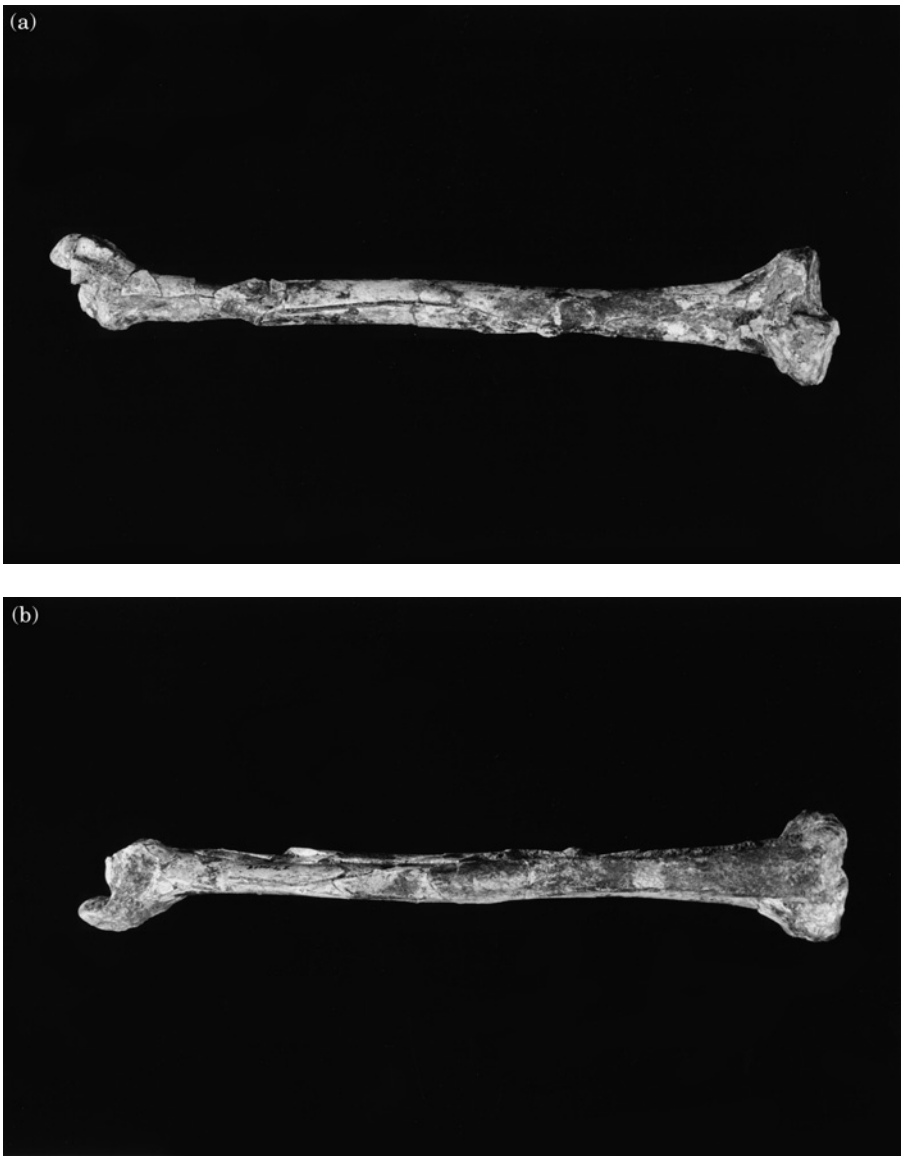

Figure 12. (a) and (b).

ventrally, and only slightly bowed in that direction. The tibial tuberosity is well marked, and the anterior aspect of the shaft distal to the tuberosity is rugose to midshaft. The medial malleolus is robust, but the morphology of the distal tibia is otherwise difficult to reconstruct due to extensive crushing. The most interesting part of the tibia in KNM-WT 39368 is its distal extremity, which exhibits an angulated medial malleolus and a prominent notch for the passage of the tendon of *M. tibialis posterior*.

Fibula. The right fibula (KNM-WT 39368 FA) is preserved. The shaft of the bone

Figure 12. (c).

Figure 12. The right tibia, KNM-WT 39368 EZ; (a) posterior view; (b) anterior view; (c) lateral view. Approximately one-half life size.

is straight, and the lateral malleolus is broad.

Comparative and functional anatomical results and discussion

Prior to the discovery and study of KNM-WT 39368, the postcranium of *T. brumpti* was known mostly from composite ''individuals'' representing animals quite widely separated in time and space. With the recognition of KNM-WT 39368, the opportunity exists to compare the anatomy of an acknowledged individual skeleton with that of composite individuals of its own species and with skeletons of other extinct and extant cercopithecid taxa.

The preserved portions of the skull of KNM-WT 39368 are, in general, very similar to those described for other specimens of *T. brumpti*. If there is one regret about the specimen, however, it is that the cranium itself or portions of it are not better preserved. The fragment of left frontal bone is the most interesting element of the cranium because its supraciliary ridge is significantly more gracile and less superiorly projecting than the prominent ''spectacle rim'' morphology seen in most specimens of *T. brumpti*. In this feature, KNM-WT 39368 most closely resembles the type specimen of *T. baringensis*, KNM-BC 2, from Chemeron, which Eck & Jablonski (1984) have suggested is representative of the basal ancestor of the *T. brumpti* lineage. The relatively gracile construction and nonprojecting morphology of the supraciliary ridge in KNM-WR 39368 also recalls that seen in most specimens of *P. hamadryas* subspecies. The supraciliary ridge also bears numerous minute foramina that were probably associated with the blood vessels supplying the bases of hair follicles. This morphology is characteristic of animals who develop supraorbital hypertrichy. The distal muzzle fragment (representing a portion of the border of the narial aperture) is small, but tantalizing in its morphology, especially, in

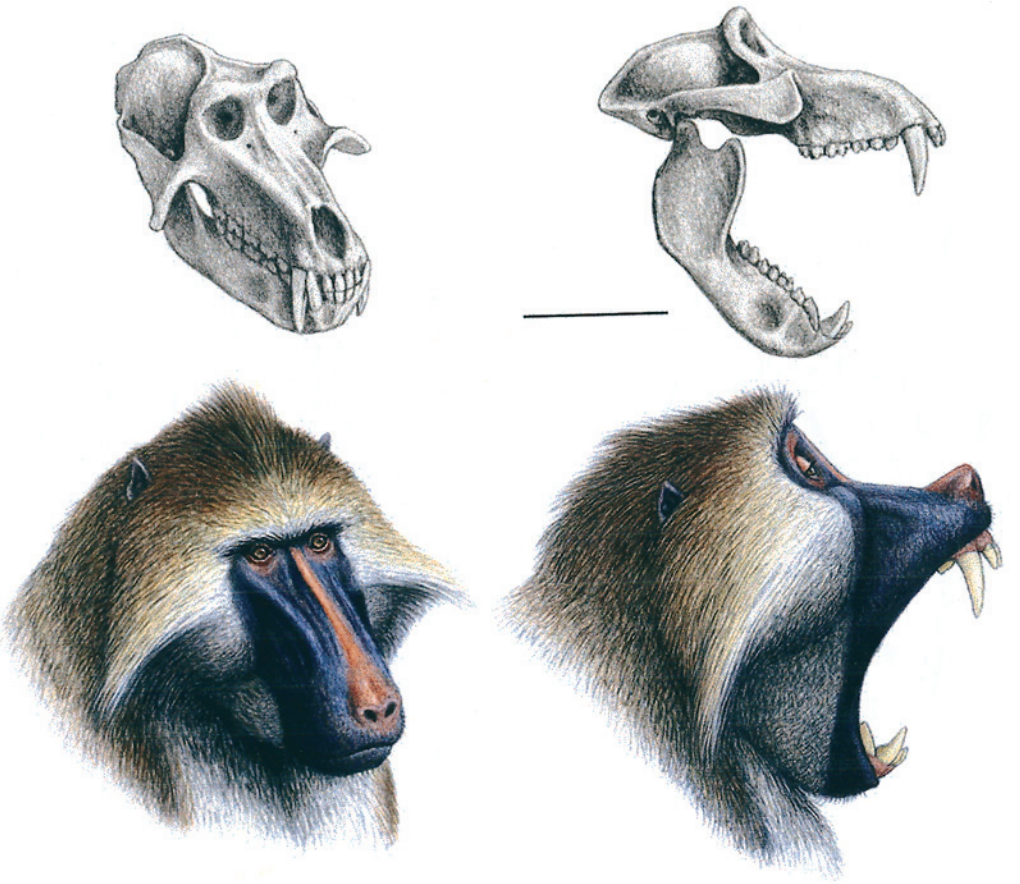

Figure 13. Reconstruction of the skull and of a male *T. brumpti*, in two views, based on a composite of cranial and mandibular specimens from the Omo and West Turkana. The nostrils are shown in an anterior position, as in modern Papionina with long muzzles and comparable nasal morphology. The skull in three-quarters view (top left) shows the anterolateral expansion of the zygomatics typical of the species, which in turn implies the presence of large *M. masseterici*, the bulk of which would be visible under the skin and fur of the living animal (bottom left). The morphology of the craniomandibular articulation, as well as other craniodental features, reflects an adaptation to wide gape displays (top right). In life, these displays would likely be emphasized by showing the light-colored eyelids, as in modern papionins (bottom right). A dark muzzle and facial mask would provide for a dramatic contrast against the light-colored teeth and gums.

its preservation of a rugose surface indicative of a highly vascularized muzzle integument. This is also seen in another probable muzzle fragment (KNM-WT 39368 DS), the anatomical placement and orientation of which cannot be determined. The anatomical evidence provided by the surfaces of the supraciliary ridge and muzzle fragments suggest that KNM-WT 39368 sported shiny, colorful skin on the surface of its muzzle and areas of hypertrichy on its face. This information was then combined with paleoenvironmental evidence of the species' preference for forest habits, and the knowledge, derived from other specimens, of *T. brumpti*'s uniquely enlarged zygomatic arches and associated chewing muscles (Eck & Jablonski, 1987; Jablonski, 1993*a*). This made possible the reconstruction of the head of KNM-WT 39368 as relatively

dramatically colored and patterned (Figure 13). This configuration would encourage visibility by conspecifics under the reduced-light conditions of a forest or forest-margin habitat, as in modern guenons and mandrills.

The mandible and mandibular dentition of KNM-WT 39368 are very similar to those of other large males of *T. brumpti*, described and compared in detail by Eck & Jablonski (1987). Its only significant departure from this condition is in the mandibular dentition, which although heavily worn, differs slightly from that seen in later representatives of the species from West Turkana or the Omo. KNM-WT 39368 presents the small incisors characteristic of *T. brumpti*. The molars of KNM-WT 39368 and other early representatives of *T. brumpti* from the Tulu Bor Member of the Koobi Fora Formation and the Lower Lomekwi Member of the Nachukui Formation are characterized by lower, more broadly based cusps with fewer enamel infoldings. Simpler molar morphology has been observed by Leakey (1993) to be characteristic of all early specimens of *T. brumpti*. This morphology, which resembles that of *T. baringensis*, appears to precede the more "typical" appearance of the species, as represented by specimens from Members C-G of the Shungura Formation of the Omo or the Upper Lomekwi Member of the Nachukui Formation. This finding parallels the intriguing description of the supraorbital margin of KNM-WT 39368, which appears to represent a more primitive condition than that of later *T. brumpti*. Both morphologies strengthen the evolutionary connection between *T. baringensis* and *T. brumpti*, and support the suggestion that the former is ancestral to the latter (Eck & Jablonski, 1984).

Quadrupedal primates exhibit variations in scapular morphology associated with preferences for an arboreal or a terrestrial habitus (Ashton & Oxnard, 1964; Roberts, 1974; Kimes *et al.*, 1981). Changes in scapular blade morphology are also linked with body size differences such that larger primates of closely related groups may have relatively wider scapulae (Roberts, 1974) without necessarily exhibiting differences in locomotor behavior. In KNM-WT 39368, the scapula is narrow, having a ratio of scapular length to width of 126·7, well within the range of terrestrial cercopithecines and terrestrially adapted colobines (Ashton & Oxnard, 1964; Birchette, 1982). Although the absolute sizes of the supraspinous and infraspinous fossae were not measured on KNM-WT 39368, the considerably greater area of the latter allies it to those cercocopithecoids, such as *Papio* and *Erythorcebus*, exhibiting large percentages of terrestrial behaviors (Roberts, 1974). Of great interest on the scapula of KNM-WT 39368 is the wide axillary sulcus that marks the lateral two-thirds of the scapula's lateral border. The interpretation of this feature is difficult. If it accommodated a large accessory slip of *M. subscapularis*, the muscle may have played a significant role in humeral abduction and rotation. The last major features of importance on the scapula are the shape and orientation of the glenoid fossa. The symmetrical piriform shape of the fossa in KNM-WT 39368 that lacks collateral indentations denotes a large area of contact between the fossa and the head of the humerus. This indicates that the fossa was largely responsible for transmission of body weight and muscular compressive forces, as it is in other terrestrial cercopithecoids (Birchette, 1982). The angle of the glenoid fossa to the scapular spine has been shown by Jolly (1965), Ashton & Oxnard (1964) and others to distinguish the scapulae of terrestrial monkeys, especially baboons, from more arboreal species. In KNM-WT 39368, the glenoid fossa is oriented laterally and the aforementioned angle is 88°, within the range of modern terrestrial baboons

(Jolly, 1965). In scapular morphology, the picture of KNM-WT 39368 is principally one of a terrestrially adapted baboon, in which fore-aft movements of the forelimb in protraction and retraction dominated. The only interesting exception to this is the large size of the axillary gutter, which may indicate that KNM-WT 39368 could engage in rather more humeral abduction and lateral rotation than is the case with most other baboons. This exception is one of several interesting anatomical oddities that denote that *T. brumpti* possesses a forelimb that is more flexible at the shoulder joint than are those of other theropiths or large papionins (Krentz, 1993).

The proximal humerus of KNM-WT 39368 presents an interesting suite of characteristics that distinguish it from those of other theropiths and *Papio* baboons, including the low degree of protrusion of the greater tuberosity above the humeral head and a deep insertion for the *M. infraspinatus* on the lateral aspect of the greater tuberosity (Krentz, 1993). The proximal prolongation of the greater tuberosity has long been related to terrestrial quadrupedalism (Savage, 1957), and is directly related to increasing the moment arm of the supraspinatus about the shoulder joint. Larson & Stern (1989) have pointed out, however, that differences in the height of the greater tuberosity more accurately reflect the role of *M. supraspinatus* as an elevator of the forelimb against gravity. They interpreted the "lowering of the tuberosity" as actually raising the head upward for the purposes of increasing overall mobility at the glenohumeral joint. The relatively small size and lack of superior protrusion of the greater tuberosity of KNM-WT 39368 is in contrast to that seen in the highly terrestrial extant papionins, *T. gelada* and *P. hamadryas* subspecies, as well as in the Plio-Pleistocene theropiths, *T. darti* and *T. oswaldi*. The prominence of the insertion of *M. infraspinatus* signifies the importance of the muscle in shoulder stabilization as well as in lateral rotation of the humerus. This insertion tends to be more prominent in arboreal species, reflecting the role of *M. infraspinatus* in enhancing shoulder stability, and less prominent in terrestrial ones in which the muscles of the rotator cuff in general tend to be relatively smaller (Krentz, 1993).

The condition presented by the distal humerus contrasts with that presented by the proximal portion of the bone. Here, the picture is more consistently of features associated with a terrestrial locomotor habitus. In KNM-WT 39368, the most important of these features is the breadth of the distal articular surface relative to the biepicondylar breadth, the retroflexion of the medial epicondyle, the narrowness of the trochlea and the steepness of its bony margins, and the distal protrusion of the trochlea. Although the latter two features appear to have been exaggerated in KNM-WT 39368 as a result of osteoarthritis, these conditions contradict those described for the distal humerus of *T. brumpti* by Krentz (1993). The index that expresses the breadth of the articular surface of the distal humerus relative to the biepicondylar width is 76·4 in KNM-WT 39368, greater than the average value of 73·4 for *Papio* baboons (Jolly, 1972) and for other theropiths studied by Krentz (1993), including his sample of *T. brumpti* (*T. gelada*=71·6; *T. oswaldi*=70·1, and *T. brumpti*=72·4). All of the theropiths, including KNM-WT 39368 cross Jolly's (1972) rubicon of 70% that distinguishes terrestrial from arboreal cercopithecids. The large size and posterior projection of the medial epicondyle bespeaks two important conditions relevant to locomotion and manipulation in KNM-WT 39368. Firstly, the large size indicates that the animal possessed large carpal and distal flexors that would have enhanced its abilities to grasp fine objects during feeding (Jolly, 1970). Secondly, the medial epicondyle protrudes more strongly

posteriorly than medially, in order to enhance the action of the pronators and flexors (Fleagle & Simons, 1982). Thus, KNM-ER 39368 appears to have possessed large carpal pronators and digital and carpal flexors, the origins of which were situated to enhance their mechanical advantage. The importance of the narrowness of the trochlea and the distal extension of the trochlear flange in KNM-ER 39368 is difficult to assess because of the arthritic pathology that appears to have accentuated their expression. Inspection of other specimens of the distal humerus of *T. brumpti* indicates, however, that the condition of KNM-ER 39368 is only a slight exaggeration of that observed in other examples of the species from Koobi Fora and West Turkana. The narrowness of the trochlea is interpreted then as an indication of the degree of sharing between the humeroulnar and humeroradial joints in the role of transmitting compressive and tensile forces across the elbow joint (Birchette, 1982). In arboreal species, the surface area of the former articulation is considerably larger than the latter, an arrangement that frees the latter to maneuver more freely in pronation and supination. The distal extension of the trochlear flange has been interpreted similarly by Jolly (1965), as a characteristic of terrestrial species which require greater elbow stability by counteracting the forces that would tend either to displace the ulna medially or the humerus laterally. In summary, the humerus of KNM-WT 39368 and other representatives of *T. brumpti* presents a suite of features, especially in the distal humerus, that are generally characteristic of terrestrial papionins, but which emphasize greater flexibility at the glenohumeral joint and strength of the digital and carpal flexors.

The ulna is a particularly informative bone in terms of providing insight into the locomotor habits of Old World monkeys. The most important features of the ulna that will be considered here are the relative length of the olecranon, the inclination of the olecranon process relative to the ulnar shaft (olecranon retroflexion), the configuration of the medial surface of the olecranon process, and the width and orientation of the articular surface of the sigmoid notch. The important features of coronoid process projection, shape of the radial notch and ulnar shaft robustness were not possible to accurately assess for KNM-WT 39368 because of pathology and damage. The relative length of the olecranon process is related to the action of *M. triceps brachii* and is considered a measure of the lever arm of that muscle (Gray, 1968). A short process permits full extension of the elbow, which increases the length of the forelimb and which, in turn, increases the length of stride. A longer olecranon process increases the leverage of *M. triceps brachii* and increases the mechanical efficiency of the muscle when the forearm is flexed (Gray, 1968; Conroy, 1974). A long olecranon process is characteristic of arboreal primates, while a relatively lower process is characteristic of terrestrial primates that normally have their forelimbs extended during locomotion (Oxnard, 1963; Jolly, 1967; Ashton *et al.*, 1976). The olecranon process of KNM-WT 39368 is long and the index expressing its relative length is 7·8, just exceeding the value of 7·6 for *Colobus* reported by Birchette (1982). Krentz (1993), utilizing a different index of relative olecranon process length, also found that *T. brumpti* had relatively longer processes than *Papio* baboons or other theropiths except for *T. darti*. This finding is curious when one considers that the olecranon of KNM-WT 39368 and other specimens of *T. brumpti* is highly retroflexed. Ulnar retroflexion has been found to consistently differentiate arboreal from terrestrial cercopithecids because olecranon process inclination is related to the different requirements of *M. triceps brachii* for maximum efficiency in climbing versus moving over a level surface (Jolly,

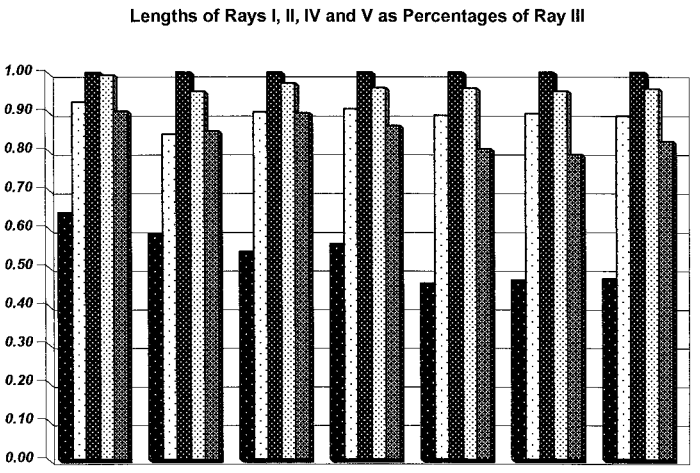

	KNM-WT 39368	T. gelada	P. h. hamadryas	P. h. cynocephalus	E. patas	C. aethiops	M. mulatta
Ray I	0.64	0.59	0.54	0.56	0.46	0.46	0.47
Ray II	0.92	0.84	0.90	0.91	0.89	0.89	0.89
Ray III	1.00	1.00	1.00	1.00	1.00	1.00	1.00
Ray IV	0.99	0.95	0.97	0.96	0.96	0.95	0.96
Ray V	0.90	0.85	0.90	0.86	0.80	0.79	0.82

Figure 14. The lengths of manual rays I, II, IV and V expressed as percentages of the length of manual ray III. Data for living species are from Etter (1973).

1967). A retroflexed olecranon process provides great mechanical advantage to *M. triceps brachii* when the forearm is already extended, as in the final part of the propulsive phase of terrestrial locomotion. The olecranon of KNM-WT 39368 exhibits an angle of retroflexion of 48°, higher than that reported for other specimens of *T. brumpti* (39·5°) (Krentz, 1993), exceeding those for *T. oswaldi* (43·6°) (Krentz, 1993), and within the range reported by Jolly (1967) for *Papio* (40–60°). The olecranon process of KNM-WT 39368 and, to lesser extents, of other theropiths is unusual in that it combines the relatively great length of arboreal cercopithecids with the extreme retroflexion of terrestrial ones. This unique combination may contribute to the tremendous alacrity shown by geladas as they ascend near-vertical cliffs in powerful bounds, from positions in which their elbows are already extended (personal observation by NGJ based on observation of video footage). In *T. brumpti*, the combination may have been related to a mode of locomotion or foraging for which there is no living analog. The medial surface of the olecranon of KNM-WT 39368, like that of other members of its species and other theropiths, accommodated a large mass of muscles

Table 6 Opposability indices for KNM-WT 39368, L865-2 (*T. brumpti* from the Omo reported by Jablonski, 1986), and other cercopithecines (as reported by Etter, 1973)

Specimen or species	Opposability index
KNM-WT 39368	69·2
L865-2	70·6*
Theropithecus gelada (n=5)	69·7
Papio h. hamadryas (n=12)	60·1
Papio h. cynocephalus (n=8)	61·7
Erythrocebus patas (n=9)	51·3
Cercopithecus aethiops (n=12)	52·0
Macaca mulatta (n=15)	52·9

*Indicates an estimated value. See Jablonski (1986) for details.

related to radial deviation of the wrist and flexion of the fingers. This pattern, which is related to grasping in arboreal species, is not seen in other terrestrial papionins. Its consistent occurrence in *Theropithecus*, however, has been convincingly linked by Jolly (1972) and Maier (1972) to extreme manual dexterity and an adaptation for manual grazing. The articular surface of the sigmoid notch in KNM-WT 39368 is narrow and resembles a twisted parallelogram, with the sides and the articular surfaces directed craniolaterally. This configuration occurs in primates that move with extended elbows, in which the angulation of the sigmoid notch facilitates straighter fore and aft movements of the forearm (Krentz, 1993). The narrowness of the sigmoid notch of KNM-WT 39368, as in the case of the humeral trochlea, indicates that the humeroulnar joint was not responsible for the transmission of most of the body weight and muscular forces, as it is in arboreal species (Conroy, 1974).

The morphology of the radius has been found to be less consistently related to locomotion than has the morphology of other forelimb elements. Few consistent differences in radial shaft curvature, robustness, diaphyseal cross-section, or neck length exist between species of highly divergent locomotor modes (Olivier & Soutoul, 1960; Jolly, 1965). Birchette (1982) and Krentz (1993) were, however, able to recognize interesting and, possibly, functionally significant differences in radial head shape and orientation in their comparative studies. Like other cercopithecids, KNM-WT 39368 exhibits an elliptical radial head, a feature that is associated with habitually pronograde animals, with limited capacities for supination. Terrestrial cercopithecids would be expected to have a more elliptical head (and higher values for its associated index) than do arboreal ones. In KNM-WT 39368, the index of radial head shape is 125, within the range of terrestrial cercopithecines (Conroy, 1974). Krentz (1993) reported that the radial head shape in *T. brumpti* was highly variable, with some individuals exhibiting quite round heads. One of us (NGJ) has also observed this and has found that rounder heads tend to be found on smaller bones, presumably from smaller individuals. Radial head shape may, thus, be related to body size or to the greater arboreal proclivities of smaller animals. The orientation of the articular surface of the radial head is also of possible functional significance. The radial head of KNM-ER 39368 and of other specimens of *T. brumpti* is only slightly angulated, an arrangement that enhances supination and pronation. In the case of the radius, as with the ulna, the two features of the radius of putative functional significance convey different messages. The elliptical shape of the radial head is generally related to higher degrees of terrestriality, while the lack of angulation of the head denotes an enhanced ability for pronation and supination of the wrist. This seeming contradiction is entirely consistent, however, with the functional picture provided by the distal humerus and ulna of KNM-WT 39368, which indicate that *T. brumpti* had an essentially terrestrially adapted forelimb that was also specialized for fine manipulation and grasping with the fingers, activities that require adept pronation and supination of the wrist.

The region of the postcranium of *Theropithecus* that has attracted the most interest and speculation has been the hand. This is because of a series of findings beginning with Napier & Napier (1967) that indicated that the living gelada had a high opposability index, and that this was related to the species' habit of manual grazing (Maier, 1972; Etter, 1973). This arrangement is produced by the relative elongation of the thumb, especially the pollical metacarpal, and the relative abbreviation of the proximal and middle phalanges of the index finger (Jablonski, 1986). In KNM-WT 39368, as in other cercopithecines, the digital formula

is III>IV>II>V>1. When the length of digits I, II, IV and V is expressed as a percentage of digit III, the greater relative length of digit I in KNM-WT 39368 and *T. gelada* is readily apparent (Figure 14). Although many indices have been devised to express the relative length of the components of the digits and the relationships of digits to one another, the opposability index of Napier & Napier (1967) remains the most economical mode of conveying the relationship between the lengths of the pollex and the index finger and their potential for opposition. The opposability indices for KNM-WT 39368 and other cercopithecines, including that of the fossil hand

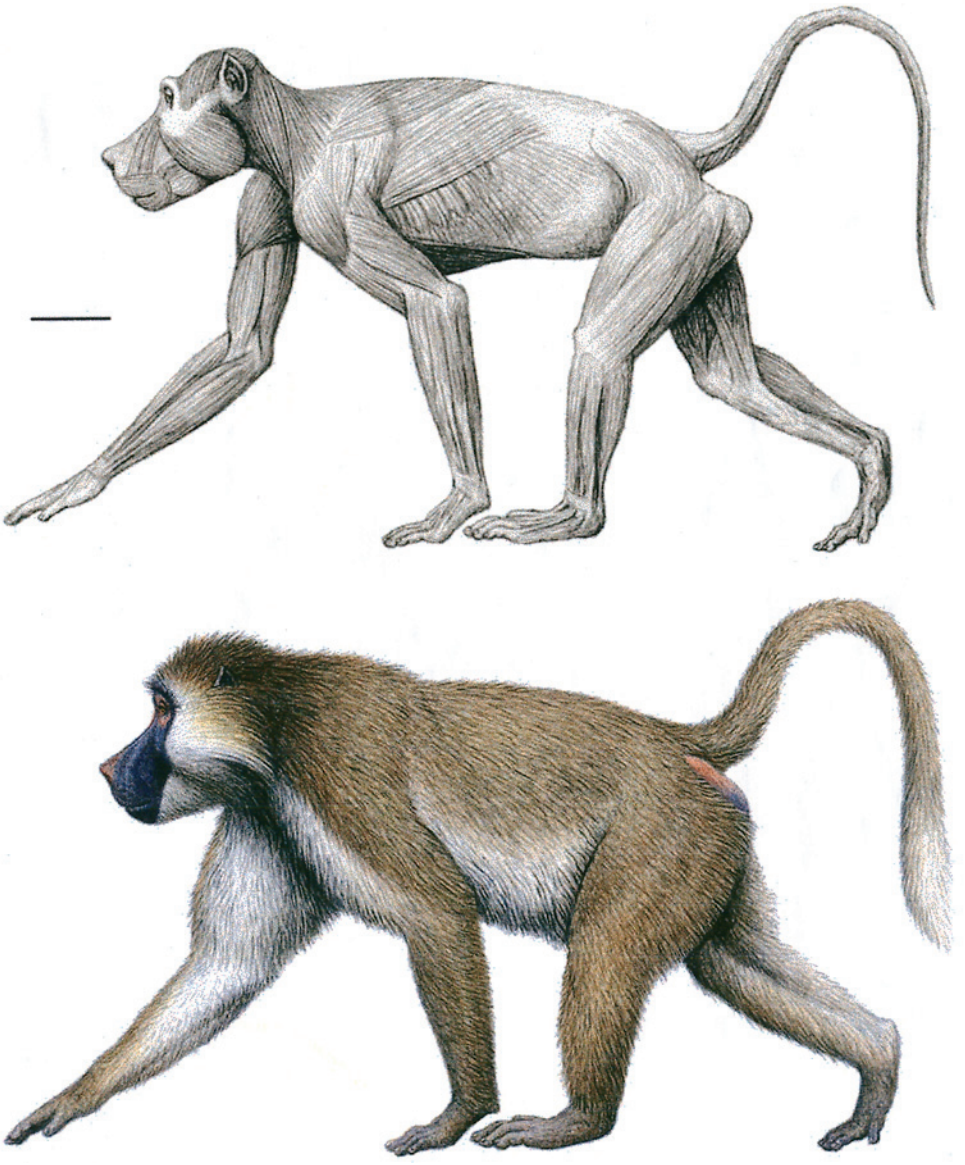

specimen of *T. brumpti* from the Omo (Jablonski, 1986), were computed as the total length of digital ray I (X 100) divided by the total length of digital ray II. The results are presented in Table 6. The opposability indices for all the theropiths are essentially the same, ranging from 69·2 for KNM-WT 39368 to 70·6 for the Omo *T. brumpti*, with an intermediate value of 69·7 for *T. gelada*. This calculation demonstrates convincingly that the high degree of opposability between the index finger and thumb is a primitive character for *Theropithecus* (Jablonski, 1986). When this information is added to that on the function of the shoulder and elbow joints in *Theropithecus*, as described here and by Krentz (1993), it is clear that the hand proportions of the genus reflect an adaptation for strong and precise pincer-like movements of digits I and II during foraging. The demonstration of very similar opposability indices in the different species of *Theropithecus* does not imply that the species had similar diets, rather that they had physically powerful precision grips that permitted them to efficiently harvest and manipulate even the smallest foodstuffs.

The final element of the postcranium of KNM-WT 39368 requiring discussion is the tibia. As mentioned above, the tibia of *T. brumpti* and other theropiths is distinguished from that of other papionins by its angulated medial malleolus and a prominent notch for the passage of the tendon of *M. tibialis posterior*. Maier (1972) and Krentz (1993) have interpreted these features as being related to greater flexibility of the foot and specifically, inversion of the foot, during foraging and locomotion. Maier (1972) reported that *T. gelada* inverts its foot much of the time while feeding, and it appears that this habit and its attendant morphology is primitive for the genus.

Although a complete roster of limb indices for KNM-WT 39368 cannot be calculated because of the absence of both femora, the brachial index can be determined. This index for KNM-WT 39368 (calculated as the length of the radius divided by the length of the humerus) is 100·9, very similar to that determined by Krentz (1993) for samples of *T. darti*, *T. oswaldi* and *T. gelada*, but significantly higher than the figure calculated by him for other specimens of *T. brumpti* (84·1), which

Figure 15. Reconstruction of the somatic musculature (top) and external appearance of *T. brumpti*, based on the skeleton of KNM-WT 39368. Information on the myology of living papionins was taken from Hartmann & Strauss (1933) and Swindler & Wood (1973), as well as from personal observations by one of us (M.A.) of a dissected specimen of *P. hamadryas hamadryas*. Reconstruction of the color pattern was based on the reference of the extant species most closely related to *T. brumpti*, that is, members of the African Papionina, which include the genera *Theropithecus*, *Papio*, *Mandrillus*, *Cercocebus* and *Lophocebus* (baboons *sensu lato* and mangabeys). A body mane like those of extant geladas and hamadryas baboons was rejected as unlikely development in a riverine baboon like *T. brumpti*. Therefore, the species was given body hair of moderate length. However, a sagittal ridge of longer hair on the top of the skull and masses of long hair growing backwards and outwards from the cheeks are common among both open-country and riverine papionins, including the mangabeys, and were, thus, incorporated into the reconstruction. A dark facial mask surrounded by light-colored fur is very widespread among papionins and other cercopithecids, and the pattern is exaggerated in such riverine species as the drill and the red-capped mangabey, both of which make extensive use of gape displays to expose their impressive canine teeth. Light-colored skin in and around the eyelids is a widespread papionin feature, while a bright band along the top of the muzzle is seen in the mandrill and in a variety of cercopithecine monkeys. The described pattern is useful for emphasizing facial expression in the low-light environment of the riverine woodland. For the body color, a moderate contrast between an olive-brown-gray dorsum and a light-colored, nearly white, ventrum was chosen. This pattern is seen in many riverine papionins, in contrast to the more uniform coloration of strictly savannah-dwelling baboons. The remarkably long tail of *T. brumpti* is here given a light tip, as in several mangabey species which also display long tails and use them in their repertoire of body language.

was based on a sample of composite individuals. When an index is calculated based on the length of the radius relative to the length of the tibia of KNM-WT 39368, a figure of 106·2 is obtained, strongly suggesting that the forelimbs of the specimen were only slightly longer than the hindlimbs.

The body size of *T. brumpti* has been estimated, using various methods, by Krentz (1993) and by Delson *et al.* (2000), resulting in estimates for male body mass ranging from 39·4 kg and 44·8 kg (Krentz, 1993) to 60 kg (Delson *et al.*, 2000). Using the equations of Delson and colleagues (2000), an estimate of body mass in KNM-WT 39368 was calculated based on humerus length (for male cercopithecines), one of the most accurate predictors of body mass. This calculation yielded an estimate of body mass for KNM-WT 39368 of 43·8 kg. *T. brumpti* is also recognized as being an extremely sexually dimorphic monkey, in its canine and P_3 dimensions, as well as in body mass (Eck & Jablonski, 1987; Delson *et al.*, 2000).

Conclusions

Careful examination and comparison of the anatomy of the partial skeleton, KNM-WT 39368, of *T. brumpti* with that of other extinct and extant cercopithecines indicates that the species is characterized by a unique mixture of postcranial features that typify both highly terrestrial and arboreal species. This is not the contradiction that it may, at first, appear. This conclusion echoes that of Krentz (1993), who found that all theropiths were distinguished by a unique suite of postcranial characters associated with forelimb flexibility and an adaptation for dexterous manipulation between the first and second digits. The main characteristics of the postcranium of KNM-WT 39368 that ally it to arboreal cercopithecines are those that are related to flexibility and enhanced mobility at the shoulder joint, enhanced capabilities for radial deviation and flexion of the wrist, and well-developed grasping abilities of the fingers. These characters are, in our opinion, imprinted on a fundamentally terrestrially adapted locomotor skeleton, in which powerful fore-aft movements of the pectoral and pelvic girdles dominated locomotion. The large bony surface areas of contact between the elements of the shoulder and elbow joints reinforce this interpretation. The anatomy of every species is an evolutionary compromise between sometimes conflicting functional demands, and that of *T. brumpti* is no exception. Its skeleton reflects the effects of natural selection operating to enhance the efficiency of the hand in foraging while retaining the overall mechanical efficiency of the limbs in terrestrial locomotion.

The diet of *T. brumpti* has been considered by several workers, based on considerations of jaw and jaw adductor morphology (Jablonski, 1993*a*) and molar tooth anatomy and microwear (Benefit & McCrossin, 1990; Teaford, 1993). Based on their examination of the lengths of molar shearing crests and other aspects of molar cusp morphology, Benefit & McCrossin (1990) predicted that *T. brumpti*, like other early theropiths, exhibited longer shearing crests and a higher potential for frugivory than *T. oswaldi*. Their inspection of the molar wear striations of *T. brumpti* confirmed this prediction by revealing an absence of deep transverse striations that may have been caused by the grit often consumed in a diet of grasses. They concluded that *T. brumpti* may have been a true papionin folivore.

Based on the anatomy described here for KNM-WT 39368, the known preference of *T. brumpti* for riverine forest or forest-margin habitats throughout its evolutionary tenure, and its presumed diet, we reconstruct the species as being a generally terrestrial—but highly dexterous—very large-bodied, sexually dimorphic, and possibly folivorous papionin. The species

appears to have been best adapted for propulsive quadrupedal locomotion over generally even ground, and yet was highly adept at manual foraging. Based on the estimates for very large body mass, especially in males, for the species, it is doubtful that it was highly arboreal, although a partly arboreal habitus may have characterized juveniles or females.

T. brumpti is known to have had a dramatic facial appearance, owing to its large zygomatic arches and greatly enlarged and anteriorly protruding *Mm. masseterici*, which facilitated the animal's gape displays (Eck & Jablonski, 1987; Jablonski, 1993*a*). Other important characteristics of the species, such as the coloration of its facial skin and hair and bodily pelage, cannot be as accurately reconstructed as those of its masticatory and locomotor systems, but still can be generally predicted on the basis of the appearance of living species today. On the basis of such analogies, we suggest that *T. brumpti* would have evolved conspicuous patterns of facial coloration, involving its muzzle skin, its facial hair, or both. The colorful and species-specific patterns of facial and perineal skin and hair seen in the modern, forest-dwelling species of *Cercopithecus* are obvious referents here, as are the brightly colored, iridescent muzzle and perineum of the large, forest-dwelling papionin, *Mandrillus sphinx*.

Thus, in its completeness, KNM-WT 39368 has given us a clearer glimpse of one of primate evolution's most intriguing and undoubtedly beautiful species (Figure 15).

Acknowledgements

We thank Wambua Mangoa and other members of the 1998 survey and excavation team at West Turkana for sighting and recovering KNM-WT 39368. Peter Gaede is thanked for drawing Figure 9, and the Fellows Fund of the California Academy of Sciences is acknowledged for providing financial support for his illustration work. Dr Francisco Pastor of the University of Valladolid, Spain, is thanked for permitting one of us (MA) to undertake a dissection of a hamadryas baboon in preparation for this reconstruction. George Chaplin is thanked for many productive discussions, and for his assistance in data recording and the identification of fragments recovered from sieving. Eric Delson and one anonymous reviewer are thanked for their constructive comments on the manuscript. Terry Harrison is warmly thanked for his constructive comments, attention to detail, and patience throughout the review process.

References

Ashton, E. H. & Oxnard, C. E. (1964). Functional adaptations in the primate shoulder girdle. *Proc. Zool. Soc. Lond.* **142,** 49–66.

Ashton, E. H., Flinn, R. M., Oxnard, C. E. & Spence, T. F. (1976). The adaptive and classificatory significance of certain quantitative features of the forelimb in primates. *J. Zool. (Lond.)* **179,** 515–556.

Behrensmeyer, A. K., Todd, N. E., Potts, R. & McBrinn, G. E. (1997). Late Pliocene faunal turnover in the Turkana Basin, Kenya and Ethiopia. *Science* **278,** 1589–1594.

Benefit, B. R. & McCrossin, M. L. (1990). Diet, species diversity and distribution of African fossil baboons. *Kroeber Anthropol. Soc. Papers* **71/72,** 77–93.

Birchette, M. G. (1982). The postcranial skeleton of *Paracolobus chemeroni*. Ph.D. Dissertation, Harvard University.

Brown, F. H., Harris, J. M., Leakey, R. & Walker, A. (1985). An integrate Plio-Pleistocene chronology for the Turkana Basin. In (E. Delson, Ed.) *Ancestors: The Hard Evidence*, pp. 82–90. New York: Alan R. Liss, Inc.

Conroy, G. C. (1974). Primate postcranial remains from the Fayum Province, Egypt, UAR. Ph.D. Dissertation, Yale University.

Coppens, Y. & Howell, F. C. (Eds) (1985). *Les Faunes Plio-Pléistocènes de la Basse Vallée de l'Omo* (*Éthiopie*). Tome 1. *Perissodactyles, Artiodactyles* (*Bovidae*). Paris: CNRS.

Coppens, Y. & Howell, F. C. (Eds) (1987*a*). *Les Faunes Plio-Pléistocènes de la Basse Vallée de l'Omo* (*Éthiopie*). Tome 2. *Les Elephantides, Proboscidea* (*Mammalia*). Paris: CNRS.

Coppens, Y. & Howell, F. C. (Eds) (1987*b*). *Les Faunes Plio-Pléistocènes de la Basse Vallée de l'Omo* (*Éthiopie*). Tome 3. *Cercopithecidae de la Formation de Shungura*. Paris: CNRS.

Delson, E. (1993). *Theropithecus* fossils from Africa and India and the taxonomy of the genus. In (N. G.

Jablonski, Ed.) *Theropithecus: The Rise and Fall of a Primate Genus*, pp. 157–189. Cambridge: Cambridge University Press.

Delson, E. & Dean, D. (1993). Are *Papio baringensis* R. Leakey, 1969, and *P. quadratirostris* Iwamoto, 1982, species of *Papio* or *Theropithecus*? In (N. G. Jablonski, Ed.) *Theropithecus: The Rise and Fall of a Primate Genus*, pp. 125–156. Cambridge: Cambridge University Press.

Delson, E., Terranova, C. J., Jungers, W. L., Sargis, E. J., Jablonski, N. G. & Dechow, P. C. (2000). Body mass in Cercopithecidae (Primates, Mammalia): Estimation and scaling in extinct and extant taxa. *Am. Mus. Nat. Hist. Anthropol. Papers* **83**, 159 pp.

Disotell, T. R. (2000). The molecular systematics of the Cercopithecidae. In (P. F. Whitehead & C. J. Jolly, Eds) *Old World Monkeys*, pp. 29–56. Cambridge: Cambridge University Press.

Eck, G. G. (1987). *Theropithecus oswaldi* from the Shungura Formation, Lower Omo Basin, southwestern Ethiopia. In (Y. Coppens & F. C. Howell, Eds) *Les Faunes Plio-Pléistocènes de la Basse Vallée de l'Omo* (*Éthiopie*). Tome 3. *Cercopithecidae de la Formation de Shungura*, pp. 123–140. Paris: CNRS.

Eck, G. G. & Jablonski, N. G. (1984). A reassessment of the taxonomic status and phyletic relationships of *Papio baringensis* and *Papio quadratirostris* (Primates: Cercopithecidae). *Am. J. phys. Anthrop.* **65,** 109–134.

Eck, G. G. & Jablonski, N. G. (1987). The skull of *Theropithecus brumpti* compared with those of other species of the genus *Theropithecus*. In (Y. Coppens & F. C. Howell, Eds) *Les Faunes Plio-Pléistocènes de la Basse Vallée de l'Omo* (*Éthiopie*). Tome 3. *Cercopithecidae de la Formation de Shungura*, pp. 10–122. Paris: CNRS.

Etter, H. F. (1973). Terrestrial adaptations in the hands of the Cercopithecinae. *Folia primatol.* **20,** 331–350.

Feibel, C. S., Brown, F.H. & McDougall, I. (1989). Stratigraphic context of fossil hominids from the Omo Group Deposits northern Turkana Basin, Kenya and Ethiopia. *Am. J. phys. Anthrop.* **78,** 595–622.

Feibel, C. S., Harris, J. M. & Brown, F. H. (1991). Palaeoenvironmental context for the late Neogene of the Turkana Basin. In (J. M. Harris, Ed.) *Koobi Fora Research Project*. Volume 3. *The Fossil Ungulates, Geology, Fossil Artiodactyles and Palaeoenvironments*, pp. 321–370. Oxford: Oxford University Press.

Fleagle, J. G. & Simons, E. L. (1982). The humerus of *Aegyptopithecus zeuxis*, a primitive anthropoid. *Am. J. phys. Anthrop.* **59,** 175–193.

Foley, R. A. (1993). African terrestrial primates: The comparative evolutionary biology of *Theropithecus* and the Hominidae. In (N. G. Jablonski, Ed.) *Theropithecus: The Rise and Fall of a Primate Genus*, pp. 245–270. Cambridge: Cambridge University Press.

Frost, S. R. (2001). New Early Pliocene Cercopithecidae (Mammalia: Primates) from Aramis, Middle Awash Valley, Ethiopia. *American Museum Novitates* **3350,** 1–36.

Gibert, J., Ribot, F., Gibert, L., Leakey, M., Arribas, A. & Martinez, B. (1995). Presence of the cercopithecid genus Theropithecus in Cueva Victoria (Murcia, Spain). *J. hum. Evol.* **28,** 487–493.

Gray, J. (1968). *Animal Locomotion*. London: William Clowes.

Harris, J. M. (Ed.) (1983). *Koobi Fora Research Project*. Volume 2. *The Fossil Ungulates: Proboscidea, Perissodactyla, and Suidae*. Oxford: Clarendon Press.

Harris, J. M. (1991). *Koobi Fora Research Project*. Volume 3. *The Fossil Ungulates: Geology, Fossil Artiodactyls, and Palaeoenvironment*. Oxford: Clarendon Press.

Harris, J. M., Brown, F. H. & Leakey, M. G. (1988*a*). Stratigraphy and paleontology of Pliocene and Pleistocene localities west of Lake Turkana, Kenya. *Contributions in Science* **399,** 1–128.

Harris, J. M., Brown, F. H., Leakey, M. G., Walker, A. C. & Leakey, R. E. (1988*b*). Pliocene and Pleistocene hominid-bearing sites from west of Lake Turkana, Kenya. *Science* **239,** 27–33.

Hartman, C. G. & Straus, W. L. (1933). *Anatomy of the Rhesus Monkey*. New York: Hafner.

Jablonski, N. G. (1986). The hand of *Theropithecus brumpti*. In (J. G. Else & P. C. Lee, Eds) *Primate Evolution*. Selected Proceedings of the Tenth Congress of the International Primatological Society, Vol. 1, pp. 173–182. Cambridge: Cambridge University Press.

Jablonski, N. G. (1993*a*). Evolution of the masticatory apparatus in *Theropithecus*. In (N. G. Jablonski, Ed.) *Theropithecus: The Rise and Fall of a Primate Genus*, pp. 299–319. Cambridge: Cambridge University Press.

Jablonski, N. G. (Ed.) (1993*b*). *Theropithecus: The Rise and Fall of a Primate Genus*. Cambridge: Cambridge University Press.

Jolly, C. J. (1965). Origins and specialization of the long-faced Cercopithecoidea. Ph.D. Dissertation, University of London.

Jolly, C. J. (1967). The evolution of baboons. In (H. Vagtborg, Ed.) *The Baboon in Medical Research*, pp. 23–50. Austin: University of Texas Press.

Jolly, C. J. (1970). The seed-eaters: A model of hominid differentiation based on a baboon analogy. *Man* **5,** 5–26.

Jolly, C. J. (1972). The classification and natural history of *Theropithecus* (*Simopithecus*) (Andrews, 1916), baboons of the African Plio-Pleistocene. *Bull. Br. Mus. nat. Hist. (Geol.)* **22,** 1–123.

Kimbel, W. H., Johanson, D. C. & Rak, Y. (1994). The first skull and other new discoveries of *Australopithecus afarensis* at Hadar, Ethiopia. *Nature* **368,** 449–451.

Kimes, K., Siegel, M. I. & Sadler, D. H. (1981). Musculoskeletal scapular correlates of plantigrade and acrobatic positional activities in *Papio cynocephalus anubis* and *Macaca fascicularis*. *Am. J. phys. Anthrop.* **55,** 463–472.

Krentz, H. (1993). Postcranial anatomy of extant and extinct species of *Theropithecus*. In (N. G. Jablonski, Ed.) *Theropithecus: The Rise and Fall of a Primate Genus*, pp. 383–422. Cambridge: Cambridge University Press.

Larson, S. G. & Stern, J. T. (1989). Role of supraspinatus in the quadrupedal locomotion of vervets (*Cercopithecus aethiops*): implications for the interpretation of humeral morphology. *Am. J. phys. Anthrop.* **79,** 369–377.

Leakey, M. G. (1993). Evolution of *Theropithecus* in the Turkana Basin. In (N. G. Jablonski, Ed.) *Theropithecus: The Rise and Fall of a Primate Genus*, pp. 85–123. Cambridge: Cambridge University Press.

Leakey, M. G., Feibel, C. S., Bernor, R. L., Cerling, T. E., Harris, J. M., Stewart, K., Storrs, G. W., Walker, A., Werdelin, L. & Winkler, A. (1996). Lothagam: A record of faunal change in the late Miocene of East Africa. *J. Vert. Paleontol.* **16,** 556–570.

Leakey, M. G., Spoor, F., Brown, F. H., Gathogo, P. N., Kiarie, C., Leakey, L. N. & McDougall, I. (2001). New hominin genus from eastern Africa shows diverse middle Pliocene lineages. *Nature* **410,** 433–440.

Maier, W. (1972). Anpassungstyp und systematische Stellung von *Theropithecus gelada* Ruppell, 1835. *Z. Morph. Anthrop.* **63,** 370–384.

Napier, J. R. & Napier, P. (1967). *A Handbook of Living Primates*. London: Academic Press.

Olivier, G. & Depreux, R. (1954). L'omoplate de semnopithéque. *Mammalia* **18,** 181–211.

Olivier, G. & Soutoul, J.-H. (1960). Les os de l'avant-bras du semnopithéque. *Mammalia* **24,** 228–258.

Oxnard, C. E. (1963). Locomotor adaptations in the primate forelimb. *Symp. zool. Soc. Lond.* **10,** 165–182.

Roberts, D. (1974). Structure and function of the primate scapula. In (F. A. Jenkins, Ed.) *Primate Locomotion*, pp. 171–200. New York: Academic Press.

Savage, R. (1957). Quadrupedal locomotion. *Proc. Zool. Soc. Lond.* **129,** 151–172.

Swindler, D. & Wood, C. (1973). *An Atlas of Primate Gross Anatomy*. Seattle: University of Washington Press.

Teaford, M. (1993). Dental microwear and diet in extant and extinct *Theropithecus*: preliminary analyses. In (N. G. Jablonski, Ed.) *Theropithecus: The Rise and Fall of a Primate Genus*, pp. 331–349. Cambridge: Cambridge University Press.

Walter, R. C. & Aronson, J. L. (1993). Age and source of the Sidi Hakoma Tuff, Hadar Formation, Ethiopia. *J. hum. Evol.* **25,** 229–240.